E. ERKAKAN METU 2014

EXPERIMENTAL INVESTIGATION OF UPLIFT ON SEISMIC BASE ISOLATORS

EVREN ERKAKAN

AUGUST 2014

EXPERIMENTAL INVESTIGATION OF UPLIFT ON SEISMIC BASE ISOLATORS

A THESIS SUBMITTED TO
THE GRADUATE SCHOOL OF NATURAL AND APPLIED SCIENCES
OF
MIDDLE EAST TECHNICAL UNIVERSITY

BY

EVREN ERKAKAN

IN PARTIAL FULFILLMENT OF THE REQUIREMENTS
FOR
THE DEGREE OF MASTER OF SCIENCE
IN
CIVIL ENGINEERING

AUGUST 2014

Approval of the thesis:

EXPERIMENTAL INVESTIGATION OF UPLIFT ON SEISMIC BASE ISOLATORS

submitted by **EVREN ERKAKAN** in partial fulfillment of the requirements for the degree of **Master of Science in Civil Engineering Department, Middle East Technical University** by,

Prof. Dr. Canan Özgen _____
Dean, Graduate School of **Natural and Applied Sciences**

Prof. Dr. Ahmet Cevdet Yalçıner _____
Head of Department, **Civil Engineering**

Assoc. Prof. Dr. Alp Caner _____
Supervisor, **Civil Engineering Dept., METU**

Examining Committee Members:

Prof. Dr. Uğurhan Akyüz _____
Civil Engineering Dept., METU

Assoc. Prof. Dr. Alp Caner _____
Civil Engineering Dept., METU

Assoc. Prof. Dr. Ahmet Türer _____
Civil Engineering Dept., METU

Prof. Dr. Ahmet Cevdet Yalçıner _____
Civil Engineering Dept., METU

Kemal Arman Domaniç _____
Bridge Engineer, Yüksel Domaniç A.Ş.

Date: 29.08.2014

I hereby declare that all information in this document has been obtained and presented in accordance with academic rules and ethical conduct. I also declare that, as required by these rules and conduct, I have fully cited and referenced all material and results that are not original to this work.

Name, Last name : EVREN ERKAKAN

Signature :

ABSTRACT

EXPERIMENTAL INVESTIGATION OF UPLIFT ON SEISMIC BASE ISOLATORS

Erkakan, Evren
M.Sc., Department of Civil Engineering
Supervisor: Assoc. Prof. Dr. Alp Caner

August 2014, 75 pages

Elastomeric rubber bearings reinforced with steel shims, are used to provide structural support in vertical direction and allow horizontal movements for the structure subjected to earthquake and thermal loads. Generally, it is known that tensile stress or uplift may occur when the structure is subjected to strong ground motion or structure have large height-to-width aspect ratio to develop a stability concern subjected to lateral loads. The main focus of this research is to investigate the change in characteristic behavior of bearings under vertical tension load and horizontal load since limited information is available on this combination of loads. For this purpose, four bearings having the same shape factor with different sizes and two other bearings are examined. They are subjected to a series of staged and cyclic loads. Shear modulus values under different vertical loads are calculated according to both TS EN 1337-3 and BS 5400 specifications separately. It is observed that shear modulus decrease with Mullin's Effect for standard bearings while decreasing in shear modulus of concave edged bearing related to strain amplitude. At the end of study, it can be stated that considerable results are obtained and this pioneering research indicate that bearings can take tension loads while subjected to horizontal loads. Still the subject needs further research and testing.

Keywords: seismic isolator, rubber, bearing, uplift

ÖZ

SİSMİK İZOLATORLER ÜZERİNDEKİ KALDIRMA ETKİSİNİN DENEYSEL OLARAK İNCELENMESİ

Erkakan, Evren
Yüksek Lisans, İnşaat Mühendisliği Bölümü
Tez Yöneticisi: Doç. Dr. Alp Caner

Ağustos 2014, 75 sayfa

Çelik plakalar ile güçlendirilmiş elastomerik kauçuk mesnetler, termal yükler ve depreme maruz kalan yapıları dikey yönde desteklemek ve yatay hareketlere izin vermek için kullanılır. Genel olarak, yanal yüklere maruz kalan yapıda kararlılık oluşturmak için yüksekliğinin genişliğine oranı fazla ya da yeryüzü hareketi çok kuvvetli olduğunda çekme kuvvetinin oluşabildiği bilinmektedir. Hala bu yük birleşimi ile ilgili sınırlı sayıda bilgi bulunması nedeniyle bu çalışmanın asıl amacı mesnetlerin çekme ve yatay kuvvetler altındaki karakteristik davranışının değişimini incelemektir. Bu nedenle, aynı şekil katsayısına ama farklı boyutlarda dört mesnet ve konkav kenarlara sahip iki mesnet incelenmiştir. Mesnetler bir seri aşamalı ve çevrimsel yüke maruz bırakılmıştır. Farklı dikey yükler altındaki kayma modülüsü her ikisi TS EN 1337-3 ve BS 5400 şartnamesi için de ayrıca hesaplanmıştır. Kayma modülüsün konkav kenarlılar için sünme miktarı ile azalırken standart mesnetler için Mullin's Effect ile azaldığı gözlenmiştir Çalışmanın sonunda, kayda değer sonuçlar elde edildiği söylenebilir ve bu öncü araştırma mesnetlerin yatay yüklere maruz kalırken gerilme yüklerini taşıyabildiğini göstermektedir. Yine de bu konu ile ilgili daha fazla araştırma ve teste ihtiyaç vardır.

Anahtar Kelimeler: sismik yalıtıcı, kauçuk, mesnet, çekme kuvveti

To My Mother

ACKNOWLEDGMENTS

First of all, I would like to express my very great appreciation to Assoc. Prof. Dr. Alp Caner, my supervisor, for his guidance, advice, criticism and encouragements throughout the research. Moreover, his patience and understanding to my personal life is admirable. He has contributed me a lot to bring the work to the current situation.

The support of Ali Naghshineh both as a researcher and a friend cannot be ignored. He has helped on overcoming the problems related with test machine. I would like to present my sincere gratitude for his efforts and support.

The technical assistance of METU Structure Mechanics Laboratory staff is gratefully acknowledged.

I present my special thanks to TÜBİTAK for financially supporting a research Project 110G093.

Finally, thanks to my beloved wife, Sedef Damla Erkakan. I am particularly grateful for her support during hard times. I appreciate her efforts.

TABLE OF CONTENTS

LIST OF TABLES

LIST OF FIGURES

LIST OF SYMBOLS

A	Plan area of EB
A_r	Area of the overlap between top and bottom bonded areas of the deformed bearing
D	Diameter of bearing
D_a	Coefficient for shear strain
d_{max}	Maximum displacement
d_y	Yield displacement
E_c	Compression modulus of the rubber-steel composite
F_x	Shear force
F_y	Yield strength of the bearing
G	Shear modulus of rubber
h_{max}	Thickness of the thickest elastomeric layer
h_{ri}	Thickness of the inner rubber layer
h_{ro}	Thickness of the outer rubber layer
h_{rt}	Thickness of the total rubber
h_s	Thickness of steel shims
K_{eff}	Effective stiffness of the bearing
K_h	Horizontal stiffness of an EB
K_s	Shear stiffness
K_v	Vertical stiffness of an EB
L	Length of a rectangular EB (parallel to longitudinal bridge axis)
n	Number of interior layer of elastomer,
S_i	Shape factor
Q_d	Characteristic strength
T_q	Total elastomeric height of bearing
V_x	Lateral displacement
W	Width of the bearing in the transverse direction
β_{eq}	Equivalent viscous damping ratio

ε_c	Vertical strain due to compression
ε_q	Shear strain
ε_1	Shear strain at first stage
ε_2	Shear strain at third stage
γ_a	Shear strain due to horizontal load
δ	Aspect ratio
σ_s	Service average compressive stress due to the total load
τ_q	Shear stress
τ_1	Shear stress at first stage
τ_2	Shear stress at third stage

ABBREVIATIONS

ASSHTO	American association of state highway and transportation officials
ASCE	American Society of Civil Engineers
BRB	Ball rubber bearing
BS	British standards
EB	Elastomeric bearing
EDC	Energy dissipated per cycle
EQ	Earthquake
HDR	High damping rubber bearing
LRB	Lead rubber bearing
NRB	Natural rubber bearing
RB	Rubber bearing
STP	Scrap tire pads

CHAPTER 1

INTRODUCTION

1.1.General

Over the last decade's major loss of lives occurred at developing countries due to poor engineering and construction practices, especially during earthquakes. To minimize these losses, the seismic performance of structures can be improved [1]. An artificial increase of the period of vibration, by means of reducing the input energy into the structure via use of special elements can improve the seismic performance.

Mostly, elastomeric rubber bearings, reinforced with steel shims, are utilized to mitigate seismic forces at bridge type of structures. The flexibility property of rubber bearing, can lengthen the structural period and decrease energy transferred to structure. The relation between acceleration and period is given below in Figure 1.1.

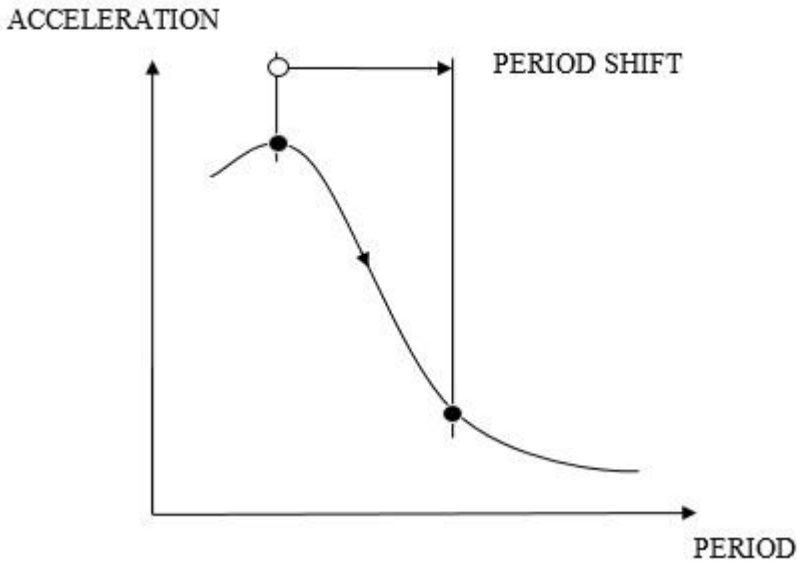

Figure 1.1: Acceleration response spectrum [2]

Seismic displacement of structure may increase as a result of flexibility. Excessive displacement can be minimized by introducing additional damper or energy dissipating mechanism. Graph showing the reduction of displacement with damping is as follows in Figure 1.2.

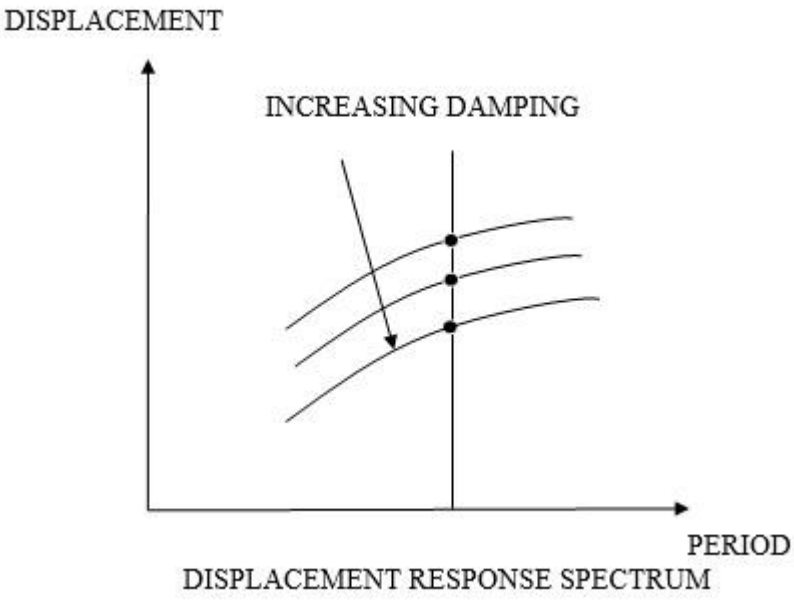

Figure 1.2: Displacement response spectrum [2]

Elastomeric rubber bearings are easy to manufacture and considerate to be durable because they have no mechanical moving parts and are more resistant to time and degradation compared to other types of isolators [3]. Moreover, viscous damping and hysteretic properties of isolators make them unsurpassed. Elastomeric rubber bearings have already exhibited a success full performance in the past earthquakes [4]. Bearing is reinforced via steel plates. Makes it stiffer in vertical direction to bear the vertical load from structure. They are usually installed at the base of buildings and at top of bridge substructures. Displacement is concentrated at the isolator level and makes the structure move as a rigid body and elastic behavior is provided above the isolators.

In general, lateral forces on seismic performance are primarily concern in mitigation of adverse effects of earthquakes. The performance of bearings under compression and shear load was typically studied. Structures like hospitals and bridges are designed to resist earthquake induced overturning moments. It has been observed that tensile stress or uplift occurs when the ground motion is very strong or structure has a large height-to-width aspect ratio [5].

It is known that each country has set a different rule or regulation to address uplift. In the following part, there are some examples with regards to limitations about tensile load determined by different standards and design manuals.

The manual of Japanese specifications for highway bridges allows up to 2 MPa tension for lead rubber bearings [4].

In New Zealand, it is limited with 3G where G is shear modulus of bearing [4].

The manual of bridge design specifications published by California Department of Transportation also denotes [6];

“Bearings shall be designed so that uplift does not occur under any combination of loads and corresponding rotation”

AASHTO LRFD (2010) indicates that [7];

“Bearings subject to net uplift at any limit state shall be secured by tie-downs or anchorages.”

According to Minimum Design Loads for Buildings and Other Structures manual of American Society of Civil Engineers [8];

“Local uplift of individual elements shall not be allowed unless the resulting deflections do not cause overstress or instability of the isolator units or other structure elements”

UNI EN 15129: Anti-seismic devices stated that [9];

“A tensile stress of up to 2G is normally sustained without significant cavitation occurring. Special connections between the isolator and the structure that remove the possibility of the vertical load on the isolator becoming tensile can be used.”

Some regulations allow tension up to a certain value as reported in the above paragraphs. In general, it is known that bearings show resistance to tensile loading. However, there are very limited studies in addressing behavior of bearing in tension and most of them are in Japanese unfortunately. Moreover, change in bearing characteristics and performance with uplift is still not clear enough. Consequently, many other studies obviously need to be carried out on effect of uplift on elastomeric rubber bearing.

1.2. Objective

No record of tension strain of rubber isolators has reported during earthquake at the investigated literature. It is known that when the ground motion is very strong, tensile stress can occur on rubber bearings. It is important to understand the behavior of rubber isolators when they are used in large aspect ratio building. Therefore, the objective of this research is to investigate the behavior of RBs subjected to tensile forces under lateral loads.

1.3. Scope

In this scope, the uplift on elastomeric bearings (RB) are studied. In the test program, various bearings with different sizes and geometry are subjected to a series of compression, tension and shear tests. The response of the RBs under combined cyclic lateral loads and axial tension loads is investigated at a series of standard tests. The results of the tests are summarized and evaluated to develop a design recommendation for structural engineers and any end user.

CHAPTER 2

LITERATURE REVIEW

2.1. General

In this chapter, selected studies about seismic isolation and Elastomeric bearings are reviewed. In addition to conventional ones, new types of bearings like BRB, STP and fiber reinforced elastomeric bearings are included. Then, effect of different factors on characteristic of bearings, studies on cases at which uplift occurs and change on behavior of EBs with tension are all described. Findings of the selected studies are summarized below.

2.2. Seismic Isolation

Buckle, I. G. and Mayes, R. L. (1990)

In this review, a short history of basic elements and performance of base isolation in worldwide was described. As known, seismic isolation was not a new concept. Prior to 1960's, despite there were lots of proposal for it, only a few of them were applicable. According to authors, development of software which made it possible for modelling systems, construction of large scale shaking tables that could simulate real earthquakes and advances in earthquake engineering facilitate improvement in seismic isolation.

In the next parts of review, application of seismic base isolation in United States, New Zealand, Japan, Italy and China were explained. Each country developed original equipment or techniques specific to conditions in their country to develop these systems. Simple and low cost solution developed for brick houses in China, an equipment that combines flexible element and energy dissipater used in New Zealand, Alexisismon which is an isolation system developed in Athens, and finally,

three different types of dampers (KP-stoppers, MS-stoppers and KK-stoppers) produced in Japan were examples for these original equipment [2].

Jangid, R. S. and Datta, T. K. (1995)

The topics and types of base-isolation were successfully reviewed by Jangid and Datta. Only the research topics were briefly given instead of a description of the full study. Following a short description, early base-isolation techniques, characteristics of laminated rubber bearing system, New Zealand bearing system, pure-friction system, resilient-friction base-isolation system, electric de France system, sliding resilient-friction system, friction pendulum system and high damping rubber bearing were explained. Analytical studies performed on base isolation such as system analyses under different conditions, accuracy of assumptions and different system modelling were listed in detail. Moreover, findings about parametric studies were given in an order since damping, yield characteristic and time period of bearing are important parameters for identification of optimum characteristics. Finally, previous experimental studies on characteristics of base isolation devices and behaviors of base-isolated buildings and application of base isolation systems were given and review ended with recommendations for further researches [10].

2.3. Studies on Elastomeric Bearings (EBs)

Takabayashi, K., Mizukoshi, K., Yasaka, A. and Iizuka, M. (1992)

When making a design, it is important to know limits of isolation system and how to establish an analytical model of structure. There are different factors affecting limit characteristics like geometrical shape, aging and loading pattern. In this research, influence of shape factor on the limit characteristics of laminated rubber bearing was studied.

Sixty-three natural rubber specimens having same diameter but different shape factors were tested. Author stated two shape factors; primary shape factor, S1 and secondary shape factor, S2 and these values were selected as 5, 20, 40 and 2, 4, 7

respectively. Different compression, tension and shear stresses and their combination were applied during tests. According to results, three types of failure were observed. Shear type became dominant at low stress levels while bending and compression types being dominant at high stress levels. In addition to these, deformation capacity decreases with smaller S1 and S2 with shear stress in constant compression load since buckling occurs at earlier stages. Under tensile and inclined loading, no difference in deformation capacity was observed with shape factor. Finally, authors recommended that S2 should be selected larger in the case of a high axial stress and noted that these results should be used for guidelines [11].

Kelly, J. M. (2002)

It is known that major loss of life occurs in developing countries like India, Turkey and South Africa. Conventional way steel reinforced elastomeric bearings are heavy, expensive and large. Thus, it should be adapted to developing countries. Author suggests that replacement of fiber reinforcement by steel plates which cause a significant increase both in weight and cost of rubber bearing. Carbon fiber is lighter and easier to process than steel plates. It also provides convenience for transportation and installation steps.

A theoretical analysis was established to add compressibility and flexibility of fibers. After that, a series of tests were carried out with a number of strip bearings having large shape factor under vertical, horizontal and cyclic loads. At the end of tests, it was seen that carbon fiber reinforced strip isolator is applicable. Theoretical results also confirmed that behavior of fiber reinforced bearing was the same as steel reinforced elastomeric bearings. Although very poor quality fiber was used for achieving low-cost aim, bearing performance was acceptable. Direction of cutting has affected the performance of bearing. Therefore, author suggests using a better cutting technique. Consequently, author stated that there were remaining uncertainties and a shaking table test should be designed for further studies. In this way, a new and attainable technology was provided [12].

Ozkaya, C., Akyuz, U., Caner, A., Dicleli, M. and Pınarbası, S. (2011)

Ozkaya et. al. developed a new type of bearing which was named as Ball Rubber Bearing (BRB). This bearing was a combination of sliding and rubber types of seismic isolators. It was provided by filling steel balls into central hole of laminated rubber bearing. It was known that energy dissipation was increased by friction and this was the case in using steel balls.

During the experiments, different parameters which affect damping property were tested. First of all, the presence of steel balls was tested. Results showed that energy dissipation capacity of bearing increased remarkably. In steel balls, temperature change was also observed because of granular friction. As another parameter, diameter of steel balls were changed (1.65, 3 and 5 mm). It was seen that frictional force decreases as contact area decreases when larger diameter steel balls were used. Similar to these, effects of central hole diameter, horizontal displacement magnitude and compression force were also tested. At the end, authors concluded that BRBs could be used in common applications because they had an easy manufacturing process and effective energy dissipation property [13].

Turer, A. and Özden, B. (2008)

Another study done on no-cost seismic base isolation mounting was performed by Türer and Özden. Tires have been produced by vulcanized steel mesh in rubber. With this structure, when a number of scrap tire pads were placed on top of each other, it was expected to see similar behavior with standard steel plate reinforced elastomeric bearing. Authors used four different well-known brands available in Turkey (GoodYear, Michelin, Pirelli and Lassa) and compared them. According to results, it was observed that STP and conventional EB had similar responses under axial loads. In addition, STP had shear modulus value between 0.95 MPa-1.85MPa changing based on the brand of tire. Because of high shear modulus value, authors recommend to use them as short span bridges and masonry houses in developing countries like Turkey, Iran, Pakistan and Chile [14].

2.4. Shaking Table Test on Base-isolated Structures

Takaoka, E., Takenaka, Y. and Nimura, A. (2011)

In this study, the ultimate behavior of structure with a high aspect ratio (equal to or/and larger than 4) was investigated with shaking table test. For this purpose, a scale model which is base-isolated via four lead rubber bearings. The aspect ratio of structure was chosen as 4 and 6 respectively. Accelerometers and displacement meters were installed at different floors of structures. As a result, the time history results of this structure and buckling behaviors of bearings showed that superstructure have three types of motion at high input levels. These are sinking type, uplift type and mixed type in which both sinking and uplift occurred at the same time [15].

Feng, D., Miyama, T., Lu, X. and Ikenaga M. (2004)

In this study, a shaking table test was performed in order to investigate hysteresis and static characteristics of bearings. According to the authors, the tensile load can easily occur in super-structures and the important thing is to know the characteristic of bearing under tension. Again a super-structure with an aspect ratio of four and base-isolated via four lead rubber bearing were targeted. During tests, four earthquakes were used as excitations. These were 1940 El Centro, 1952 Taft, 1968 Hachinohe and 1995 Kobe. After 55 test cases in total, there were tension in 14 cases and the maximum tensile stress reached was 2.2 MPa. Despite the tensile stress applied on bearing, it was observed that the hysteresis loop stood stable. A routine static test was performed both before and after shaking table test in order to be able to observe how characteristics changed. Finally, it was determined by the authors that yield load changed -8%, so there was a little change when number of tests were considered [5].

Maseki, R., Nagashima, I. and Hisano M. (2000)

A new type of isolation system was introduced by the authors as a combination of sliding bearings and laminated bearings. The resonance period of buildings get

increased by use of sliding bearing since sliding bearing keeps sliding during the earthquake different than laminated rubber bearing. It was important to understand the stability of building and new isolation system against overturning moment at which uplift and tensile stress observed in bearings.

In order to test the performance of isolation system, a frame model of building with an aspect ratio of five was tested by the records of 1940 El Centro, 1968 Hachinohe and 1995 Kobe earthquakes. Four middle columns and four corner columns were isolated by laminated rubber bearing and sliding bearings respectively.

At the end of several tests, authors determined that tensile stress and uplift occur when excitation was very strong. Nevertheless, building was stable and isolation system preserves the sufficient isolation performance. A simulation of frame model was also accurately performed by considering uplift and tensile stress in bearings [16].

2.5. Studies on Elastomeric Bearing in Tension

Iwabe, N., Takayama, M., Kani, N. and Wada, A. (2000)

Iwabe and et. al. investigated the change on behavior of three types of laminated rubber bearings before and after tension loading. These types were (1) natural rubber bearing, (2) high damping rubber bearing and (3) lead-plug rubber bearing. For all specimens, total number was 16, secondary shape factors were 5. At the beginning of tests, pre-loading was applied to high damping rubber bearing to stabilize its hysteresis behavior. After that, a series of compression and tensile loading companied a shear strain set to 100 and 200% were performed. Moreover, tensile strain was changed between 5, 10, 25, 50, 75 and maximum 100% values.

According to test results, linear behavior of hysteresis loops lost after 10% tensile strain. It was explained with the decrease of tensile rigidity of bearing after some point. It was observed that tensile load increases as shear strain increases because of strain hardening. Furthermore, there was an inverse ratio between tensile strain and tension stiffness in most cases and it could be explained with the generated cracks in

the rubber material. It was also supported that displacement in the hysteresis loop is increased under load control, after maximum tensile strain was reached. Although it was obvious that internal cracks occur in rubber, there was no significant change in compression and shear characteristics. Lastly, bearings did not rupture even in 100% tensile strain and 200% shear strain. It should be indicated that opposite and unexpected results were also obtained with different specimens during experiments.
Hereof, authors noted that it was difficult to explain simply why differences occur between samples subject to same experiments and conditions since it was obvious that cause of difference was related to rubber property. Moreover, flange plate deformation and thickness of cover layer should be regarded as effective parameters [17].

Yang, Q. R., Liu, W. G., He, W. F. and Feng, D. M. (2010)

In this paper, tensile stiffness and deformation model of laminated rubber bearings were researched. Authors suggest double stiffness and original stiffness models to describe tension properties of bearings and establishing equations. Before establishing new theories, some assumptions were made. These assumptions were; in initial state, Poisson ratio is equal to 1, it obeys elastomer's incompressible assumption, stress distribution is same in both tension and compression state and vertical tensile modulus is less than (two tenths) its compression modulus. In addition to these, authors proposed that yield strain should be 3% to be able to use suggested double stiffness model used to analyze relation between nonlinear tensile stress and strain.
In order to verify new models, tension and deformation tests carried out with natural rubber bearings and lead rubber bearings having second shape factor equal to 4.8 and 5. Tests were performed with pure tension and shear tension. 0 ~ 250 % shear strain values and 1 ~ 2 N/mm^2 stress levels were chosen. Tests were divided to two sections that are equal and less than 1.2 N/mm^2 and more than 1.2 N/mm^2 stress levels used to observe effect of tensile strain.

Consequently, obtained results have shown that assumptions were suitable to suggested equations and analysis methods. New concepts to describe stiffness property and tensile deformation was suitable [18].

Mangerig, I. and Mano, T. (2009)

Mangerig and Mano examined that influence of tension on different rubber bearings (like occurring cavities) and how its characteristics change with. In this review, it was summarized that all types of bearings (NRB, HDR and LRB) show some resistance to uplift. Although this was obvious damage from cavitation by reason of tensile loading, natural rubber retains its characteristics. On the other hand, there is a loss of both tensile and compressive stiffness after high damping rubber bearing was subjected to tension. In other words, Mullin effect has more impact on HDR. For lead rubber bearing, reduction in damping is the case. According to authors, there can be a permissible tensile stress level for both natural and high damping rubber bearings. However, this value should be determined more delicately for HDR. Japanese specifications for highway bridges allow up to 2MPa tension for lead rubber bearings. Authors suggested the reconsideration for this value due to failure of LRB under tension and 175% shear strain. In addition to these, authors also mentioned that more parameters should be taken into account, like deformation of flanges, bearings having a hole in the center and fatigue aspect of rubber. Finally, they suggested further research to determine the resistance of rubbers to tension [4].

Dorfmann, A. (2003)

Dorfmann concerned with loss of stiffness and stress softening after a series of loading and un-loading cycles above a critical value in tension because of formation of cavities in rubber. Since it was not accurate enough when it modeled as hyper-elastic material, author suggests adopting pseudo-elasticity model in order to incorporate inelastic characteristics of rubber.

Author noted that above a critical point of tension loading (5G/2 based on nonlinear theory), propagation of cavitation damage starts in the center of rubber and stress

distribution becomes highly non-uniform. At constant strain, considerable reduction was observed in tensile stress level during cycles. This difference was the biggest at first cycle and become lesser after each cycle. Moreover, in the case of constant loading, residual volumetric strain was observed and its major and permanent part occurred in the first cycle again. Hence, author emphasized that most of cavities occur at first cycle.

In order to take into account residual volumetric strain and dilatational stress softening described above, author establishes a model based on pseudo-elasticity model. In this way, deformation of material was also included. Obtained results show that model is suitable for this purpose [19].

2.6. Studies on Uplift-restraint Instruments

Griffith, M. C., Aiken, I. D. and Kelly, J. M. (1990)

In this study, analysis and tests for a new displacement-control and uplift-restraint device were described. It was known from previous shaking table tests that uplift occurs in the case of an earthquake in medium-rise buildings. A test setup (a nine-story steel frame model) was prepared and isolated with lead-rubber bearings having central hole at corner columns. Frame model was tested both free-to-uplift and uplift-restrained which device was inserted into bearing conditions. During test three different earthquake motions (Imperial Valley-1940, Bucharest-1977 and Mexico City-1985 Earthquakes) were used. At the end of tests, results showed that device does not only prevent uplift but also limits horizontal displacement of structure. It was seen that vertical acceleration was also reduced to 0.3 g from 1 g. According to authors, device could be used to provide a fail-safe isolation system successfully [20].

CHAPTER 3

TEST SET UP

3.1. General

Information about test equipment and properties of EBs used in tests are given in this chapter. Design equations of the EBs are based on AASHTO, LFRD Bridge Design Specification, 2010 [7].

3.2. Test Equipment

Two test equipment are used for seismic isolation systems during tests. Both of them are located at the Structural Mechanics Laboratory of Civil Engineering Department, METU. New equipment is constructed via republic of Turkey Ministry of Transport Maritime Affairs and Communication. Both equipment can apply vertical load on bearings at both directions. Meanwhile, they can apply axial load at required stress levels combined with cyclic shear force. Machines are portable which means that they are not fixed onto the ground. General view of old equipment is given in Figure 3.1 and new equipment is given in Figure 3.2.

As noted before, load and displacement controlled experiments can be conducted in both directions. Load capacities of old and new test machines are 3000 kN, 4000 kN in vertical direction and 500 kN, 1000 kN in horizontal direction respectively. Hydraulics of old equipment is able to resist 300 bars. Two different load cells are utilized to measure the loads on bearings. The maximum diameter of bearing which can be tested with old test equipment is 360 mm. With old test machine, tests are conducted by manual control. New test equipment can reach maximum 500 mm/min in the horizontal direction. Controls are performed in both directions separately via two independent computers. Computers use a software called as DOPE test center version 2.29.1.0. The maximum size of bearing which can be tested with the new test equipment is 600x600x180 mm.

Figure 3.1: General View of the Old Testing Equipment

Figure 3.2. General View of the New Testing Equipment

3.3. Elastomeric Bearings (EBs)

Rubber is produced by a complex chemical reaction and contains many additives like cross-linking agent, vulcanization agent and accelerators. Then, un-vulcanized thin steel plates and rubber layers are placed in a mold. They are vulcanized under certain pressure and temperature. In this way, steel plates bound to rubber. Finally, a rubber layer is covered to protect internal steel layers from corrosion.

There are six different types of bearings used in tests. These are named as O-15, O-30, M-20, M-30 and C-15, C-30. The first character of the specimen's name (O and M) shows the manufacturer name and C shows the type of the specimen. There is also a numeral as the second character. It shows the diameter of bearing in cm. For example, "M-30" denotes the bearing of the Maurer manufacturer with a 30 cm diameter.

Properties of bearings are listed in Table 3.1-3. O-15, O-30, M-20 and M-30 type EBs have the same shape factors but different sizes. They are manufactured by Özdekan Kauçuk A.Ş. Ostim/Ankara and Maurer separately. Since C-15 and C-30 bearings have totally extraordinary shape, talking about their shape factor is not possible. It is manufactured by only Özdekan Kauçuk. Views of C-15 and C-30 bearing are presented in Figure 3.3. No aging process has been applied to the bearings.

Table 3.1: Sizes of the Test Bearings manufactured by Özdekan Kauçuk.

Bearing	O-15	O-30
D (mm)	150	300
h_{ri} (mm)	4	8
h_{ro} (mm)	2	4
h_s (mm)	3	3
h_{rt} (mm)	35	55

where:

D= diameter of circular bearing

h_{ri}= thickness of the inner rubber layer

h_{ro}= thickness of the outer rubber layer

h_{rt}= thickness of the total rubber

h_s= inner steel shim thickness

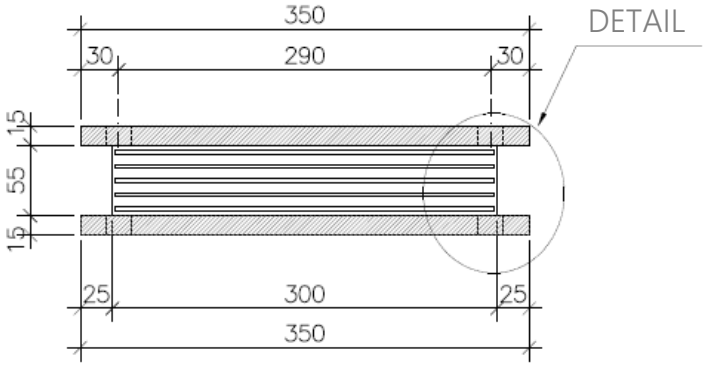

(a)

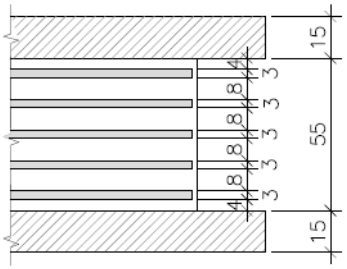

(b)

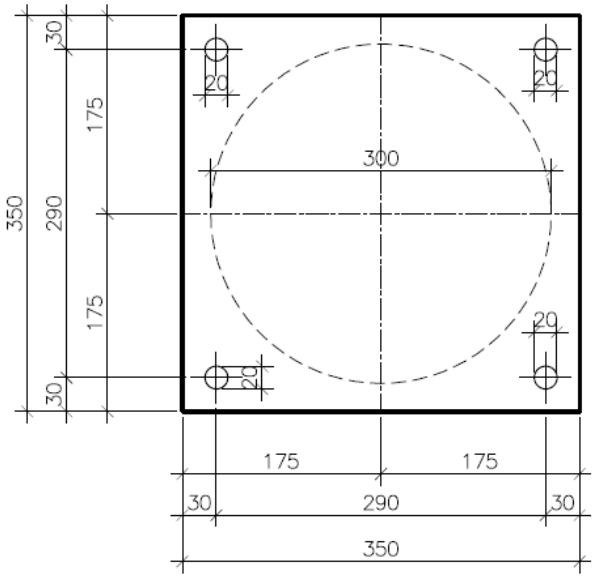

(c)

Figure 3.3: Three Different Views of the Test Bearing (O-30)

(a) Front, (b) Detail and (c) Plan View

Table 3.2: Sizes of the Test Bearings manufactured by Maurer.

Bearing	M-20	M-30
D (mm)	200	300
h_{ri} (mm)	5.4	8
h_{ro} (mm)	2.7	4
h_s (mm)	3	3
h_{rt} (mm)	42	55

where:

D= diameter of circular bearing

h_{ri}= thickness of the inner rubber layer

h_{ro}= thickness of the outer rubber layer

h_{rt}= thickness of the total rubber

h_s= inner steel shim thickness

Bearing design is evaluated per AASHTO LRFD 2010, Section 14.7.6 [7].

The shape factor of the circular bearing without holes is:

$$S_i = \frac{D}{4h_{max}} = \frac{300\ mm}{4 \times 8} = 9.375 \qquad (3.1)$$

Where h_{max} is thickness of thickest elastomeric layer and D is diameter of the loaded surface of the bearing

Bearing design is partially evaluated per AASHTO LFRD 2005 Section 14 [21].

Stability of O-15 bearing is checked:

Check if $2A \leq B$

$$A = \frac{\frac{1.92h_{rt}}{L}}{\sqrt{1 + \frac{2L}{W}}} \qquad (3.2)$$

$$B = \frac{2.67}{(S + 2.0) \times \left(1 + \frac{L}{4.0W}\right)} \qquad (3.3)$$

for circular bearings W = L = 0.8D:

$$A = \frac{\frac{1.92(20mm)}{0.8(150mm)}}{\sqrt{3}} = 0.185$$

$$B = \frac{2.67}{(11.375) \times (1.25)} = 0.188$$

So, results showed that 0.37 > 0.188 where 2A > B. Therefore, further investigation is required as indicated in specification.

In this instance:

$$\sigma_s \leq \frac{GS_i}{(2A - B)} \qquad (3.4)$$

$$\sigma_s \leq \frac{1 \times 9.375}{(0.37 - 0.188)}$$

$$\sigma_s \leq 51.51\ MPa$$

Where σ_s means service average compressive stress.

Also,

$$\gamma_a = D_a \frac{6\sigma_s}{E_c}$$

E_c is compression modulus and it can be expressed in the below equation:

$$E_c = 6GS_i \qquad (3.5)$$

So,

$$\gamma_a = D_a \frac{\sigma_s}{GS_i} \qquad (3.6)$$

$$\gamma_a = 0.11\sigma_s$$

In which, D_a is equal to 1 for circular bearings and γ_a is shear strain due to horizontal load.

Related to this value, reinforcement of bearing can be estimated;

$$h_s \geq \frac{3h_{max} \times \sigma_s}{F_y} \qquad (3.7)$$

$$h_s \geq \frac{3(4\ mm) \times \sigma_s}{2.1}$$

$$h_s \geq 5.71\sigma_s$$

Vertical strain value under compressive stress may be calculated as:

$$\varepsilon_c = \frac{\sigma_s}{6GS_i^2} < 0.07 \qquad (3.8)$$

$$0.002\sigma_s < 0.07$$

Essential features of bearings are listed in tables which are given in Appendix D with Table D.1-2.

As indicated before, C-15 and C-30 bearings don't have a specific shape factor (primary or secondary) since they have totally extraordinary shape. Their properties are given below in Table 3.3.

Table 3.3: Sizes of the Test Bearings manufactured by Özdekan Kauçuk.

Bearing	C-15	C-30
D (mm)	150	300
h_{ri} (mm)	4	8
h_{ro} (mm)	2	4
h_s (mm)	3	3
h_{rt} (mm)	35	55

where:

D= diameter of circular bearing

h_{ri}= thickness of the inner rubber layer

h_{ro}= thickness of the outer rubber layer

h_{rt}= thickness of the total rubber

h_s= inner steel shim thickness

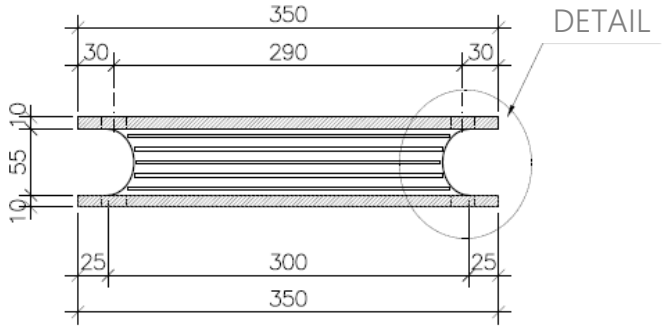

(a)

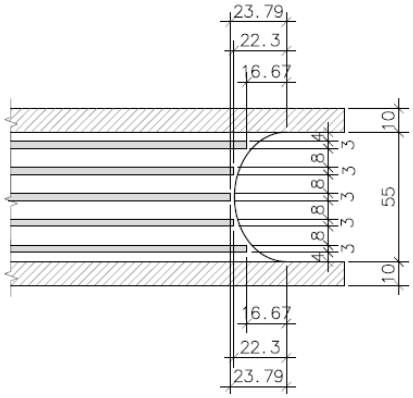

(b)

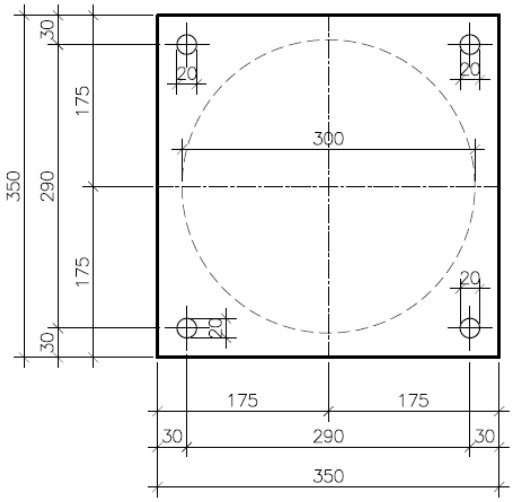

(c)

Figure 3.4. Three Different Views of the Test Bearing (C-30)

(a) Front, (b) Detail and (c) Plan View

3.4. Mechanical Properties of Elastomeric Bearings (EBs)

The mechanical properties of EBs are given and described below. Isolation systems dissipates the energy by hysteretic or viscous properties. In this study, hysteretic energy dissipation is considered while shear modulus and damping properties of bearings are calculated. The idealized force-displacement hysteretic response is presented below in Figure 3.5.

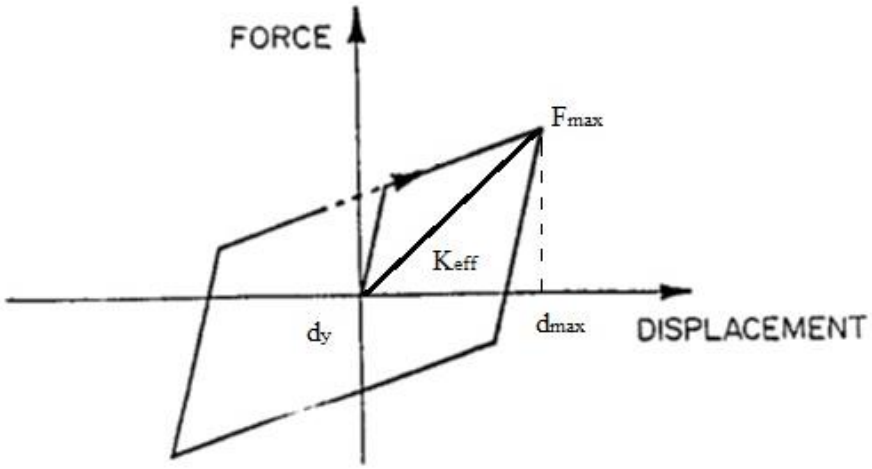

Figure 3.5: Force-displacement hysteretic response

Where d_y is yield displacement, d_{max} is maximum bearing displacement, F_{max} is maximum force and K_{eff} is effective stiffness.

Horizontal stiffness:

$$K_h = \frac{GA}{h_{rt}} \qquad (3.9)$$

Where A is plan area of EB, G is shear modulus of rubber and h_{rt} is total rubber thickness.

Vertical Stiffness is:

$$K_v = \frac{E_c A_r}{h_{rt}} \qquad (3.10)$$

Where A_r is the area of the overlap between top and bottom bonded areas of the displaced bearing [22].

CHAPTER 4

TEST METHOD

4.1. General

In this chapter, information about test method, investigated stress levels, test cases and planned test schedule are given. Tests are performed at laboratory temperatures. In the following, bearings are placed between the hydraulic jacks, compression and tension loads are applied via test equipment and end of measurement its data is plotted as load vs. displacement. Full size of two identical EBs is tested in pairs during tests.

4.2. Investigated Compressive and Tensile stress Levels

The difference between the structural response of bearings which is subjected to staged and cyclic loads under compression and tension are investigated. All bearings are tested at same stress levels to be able to observe and compare how damping ratio and shear modulus change with material property and design.

The stress level is chosen based on AASHTO specification. It is indicated that the minimum target design level is 3.5 MPa for axial compressive stress. In order to observe the effect of tensile stress on bearing, stress levels are divided into two parts as low stress level (1 MPa) and high stress level (2 MPa). The forces are computed based on the cross-sectional surface area of the bearing. The investigated stress levels with applied test type are presented below in Table 4.1.

4.3. Test Cases

Two bridge bearings which have same size are placed between plates and fixed with bolts to test machine framing. First, static compression load which is equal to 3.5 MPa is applied by hydraulic jacks. Then, the moveable middle plate is sheared to make a fully cyclic load under 3.5 MPa compression. Testing speed is chosen as 39

mm/s for O-30 bearing and 49 mm/s for O-15 bearing. This type of test is typically referred as full scale shear test [23]. This step is called as pre-conditioning or preparation stage. It is assumed that the bearing response is essentially repeatable and additional stress softening becomes negligible after this loading–unloading cycle.

After that, RBs are subjected to deform 100% of their height at earthquake state tests. It is assumed that all test conditions are earthquake state otherwise indicated because of the fact that tensile stress occurs during an earthquake. For BS 5400, RBs are subjected to displacement which is equal to 100% of their height at five steps. Approximately one minute waiting is performed in order to provide sudden creep of bearing at each step. For TS EN 1337-3, there is no waiting between steps. Finally, three fully reverse cyclic loads are applied to BRs which is equal to 100% of their height.

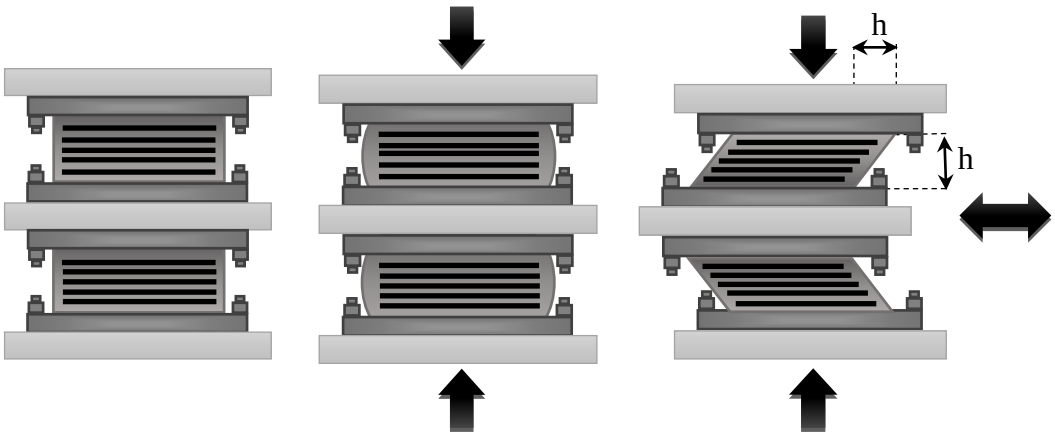

Figure 4.1: View of RBs at (a) normal state (b) under compression (c) at EQ state

At second part of the test, same procedures which are described before are repeated under 1 MPa and 2 MPa tensile stresses. A view of bearings under compression and tensile stresses are presented in Figure 4.1 and Figure 4.2 respectively. Photographs taken during tests are given in Figure C.1-5 at Appendix C.

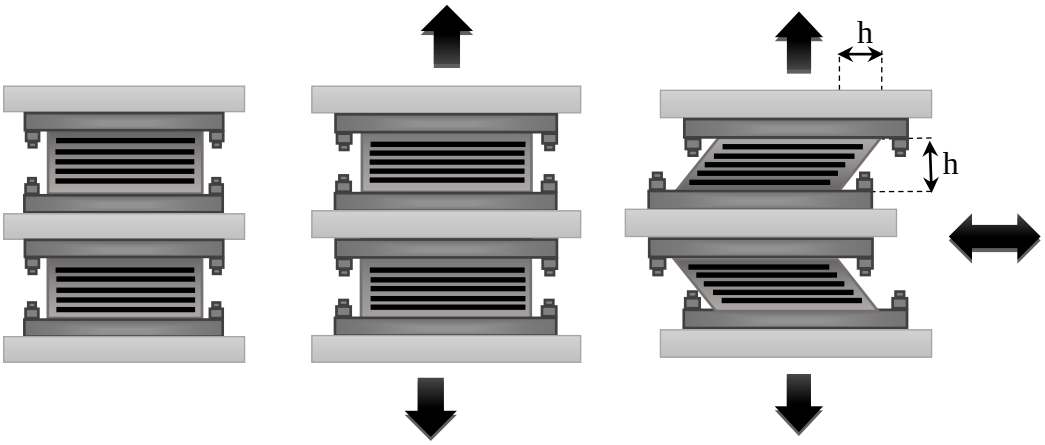

Figure 4.2: View of RBs at (a) normal state (b) under tensile stress (c) at EQ state

One of EBs (O-15) is chosen to investigate its behavior under pure tension. For this purposes, tensile load is applied till rupture without horizontal displacement. Summary of test types, compression, tensile stress and shear tests are listed in Table 4.1.

Table 4.1: Summary of compression, tensile stress and shear tests

Test Type	Compressive stress (MPa)	Tensile stress (MPa)	Lateral displacement (mm)	Number of cycles	Number of Stage
Preparation	3.5	-	±35, ±55, ±42	1	-
Staged	3.5	1, 2	+35, +55, +42	-	5
Cyclic	3.5	1, 2	±35, ±55, ±42	3	-
Rupture	-	Max.	-	-	-

4.4. Test Schedule Plan

It is aimed to apply same conditions at all tests. Due to the difference between the manufacturing dates of bearings, there cannot be a formed and applied test schedule. However, tests are performed with the following sequence that is listed in Table 4.2.

Table 4.2: Test Schedule

Step	Bearing Name	Test Type	Load
		Preparation	
1	O-15	Staged Cyclic	-3.5 MPa
2	O-15	Staged Cyclic	1 MPa
3	O-15	Staged Cyclic	2 MPa
4	O-15	Rupture	max.
		Preparation	
5	O-30	Staged Cyclic	-3.5 MPa
6	O-30	Rupture	max. - failed
		Preparation	
7	M-20	Staged Cyclic	-3.5 MPa
8	M-20	Staged Cyclic	1 MPa
9	M-20	Staged	2 MPa - failed

Table 4.2 (continued): Test Schedule

		Preparation	
10	M-30	Staged Cyclic	-3.5 MPa
11	M-30	Staged	1 MPa - failed
		Preparation	
12	C-15	Staged Cyclic	-3.5 MPa
13	C-15	Staged Cyclic	1 MPa
14	C-15	Staged Cyclic	2 MPa
		Preparation	
15	C-30	Staged Cyclic	-3.5 MPa
16	C-30	Staged Cyclic	1 MPa
17	C-30	Staged Cyclic	2 MPa

As seen on table, tensile load cannot be applied to O-30, M-20 and M-30 bearings fully. The reason behind this is that the tensile force needs to be applied to O-30 bearing exceeding the limits of instrument. Maximum tensile force which can be applied is too low and needed tensile force is equal to four times of force needed for O-15 bearing (~71 kN) since force is a function of cross sectional area of bearing. During the pure tension test, deformation occurs in outer plates where bearings connected to test machine framing with bolts before rubber are ruptured.

Photographs taken during pure tension test (start, bending of outer plates and failure stages) of O-30 bearing is given in Appendix C with Figure C.13-15.

The other cause, outer plates are not vulcanized to surface of bearings (M-20 and M-30) by manufacturer. It is tried to bond plates and bearing together with cold bonding. However, while 2 MPa tensile load applied to M-20, bearing failed at the point where bearing and plate bonded each other. This failure is repeated at 1 MPa stress level during tension test of M-30 bearing. It shows that cold bonding is not as reliable as vulcanization process since bearings has little resistance against tensile force when cold bonding is applied to them.

CHAPTER 5

SUMMARY OF RESULTS

5.1. Summary of Results

Six seismic isolators in different sizes but same shape factor and concave shaped seismic isolators are tested at a compressive and two different tensile stress levels. As a result of this, the influence of compression and tension on behavior of the bearings is investigated and compared. In this purpose, size of bearings, tensile and compressive stress levels and test cases change from one test to another.

As indicated before, all of cyclic tests are performed for the earthquake state in the experimental stage which means 100% lateral displacement. Tests of O-15 and O-30 bearings are performed via old instrument while the others are tested by new instrument. Negative sign (-) means compression and positive sign (+) means the tensile load.

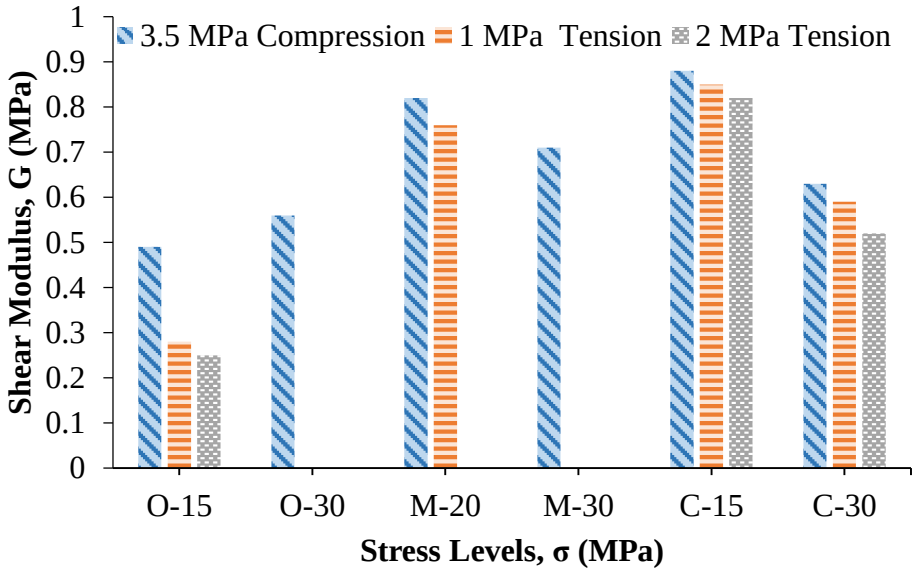

Figure 5.1: Comparison of shear modulus values calculated via TS EN 1337-3 specifications at -3.5 MPa, 1 MPa and 2 MPa stress levels

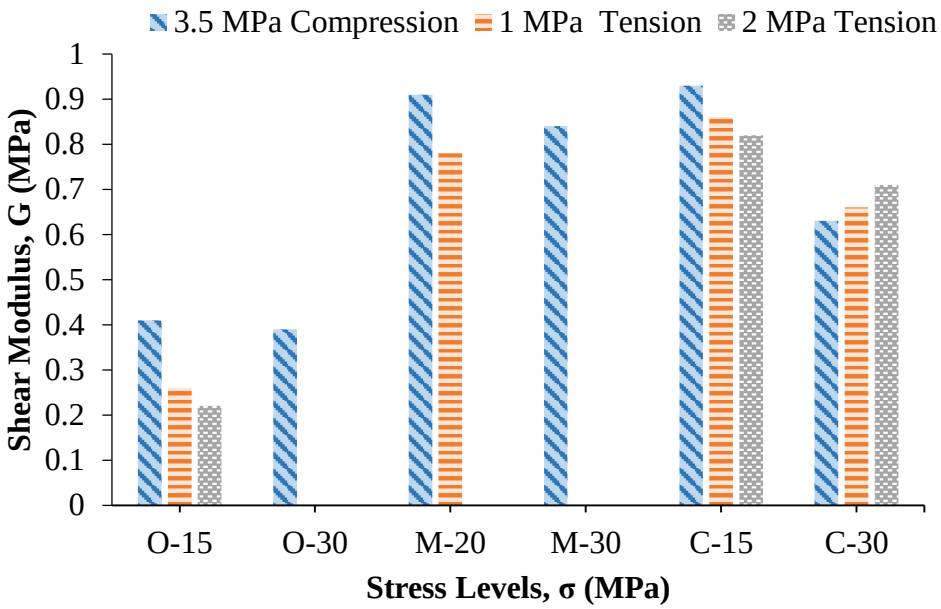

Figure 5.2: Comparison of shear modulus values calculated via BS 5400 specifications at -3.5 MPa, 1 MPa and 2 MPa stress levels

Shear modulus are calculated according to both TS EN 1337-3 and BS 5400 separately and calculated values are given above in Figure 5.1-2 and Table 5.1-3, respectively. Results show that behavior of standard bearings, having same shape factor, does not change by changing calculation method although there are some differences between them. For example, it is seen that both shear modulus values are decreased when tensile force is applied to bearing. Moreover, it decreases further as tensile stress increases. It is also seen that shear modulus increases as size of bearing increases.

However, for C-30 bearing, shear modulus values are very different from each other. When calculations are made using TS EN 1337-3 specification, shear modulus decreases as tensile stress increases but if calculations are done via BS 5400 specification, shear modulus increases while tensile force increases. In other words, behavior of bearing under tension changes by changing calculation and test method. Actually, it is expected that shear modulus decreases with tension and the reason of this is explained in the following pages.

As seen on Figure 5.1-2, shear modulus values of O-15, M-20 and C-15 bearings decrease with tension. Cause of decrease is able to be explained by Mullin's Effect. Rahim and Kamarudin studied how shear modulus change and according to authors, shear modulus decreases with Mullin's Effect [24]. This phenomenon can be described briefly as follows:

Rubber is a polymer consisting of chains of monomer compounds positioned in an irregular manner. When it is deformed by exposure to compression, tension or shear stress, chains start to locate parallel arrangement during the deformation which is denoted as crystallization. At crystallization stage, rubber becomes stiffer but weak cross-linking bonds start to break or untangling with further deformation and stiffness decrease. After all, the shear modulus decreases by the decrease in the stiffness (rigidity) of rubber.

Additionally, reduction in shear modulus can also be explained by stress softening as a result of Mullins effect. It is known that shear modulus is highly related to strain amplitude [25]. When stress softening occurs under constant tensile force, it causes an increase in strain and shear modulus decreases accordingly [17].

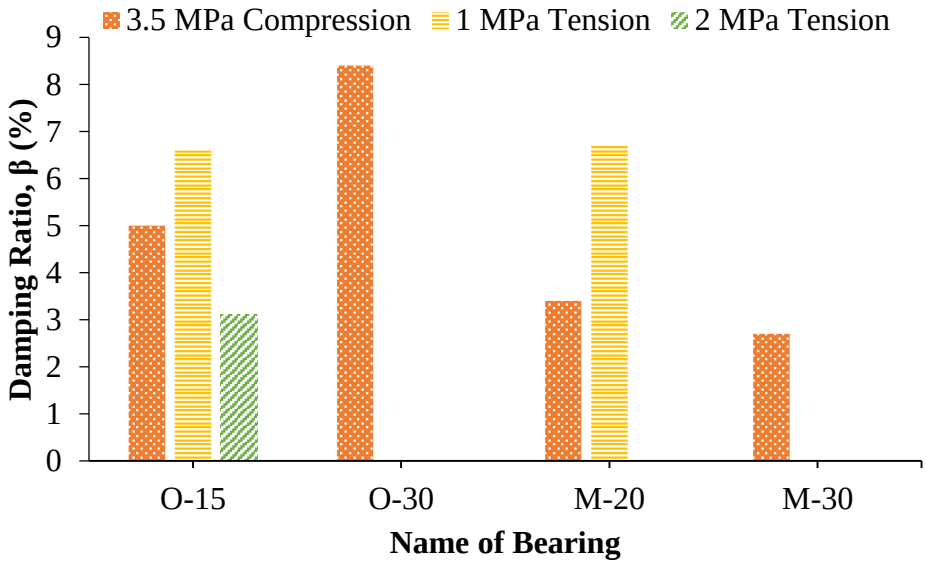

Figure 5.3: Comparison of percentage of damping of bearings under -3.5 MPa, 1 MPa and 2 MPa stress levels

Even if they have same hardness, stiffness of bearings may be different. Another explanation is done by Arditzoglou et al. as follows;

"Two elastomers of the same hardness obtained from two different rubber manufacturers will not have the same shear modulus values because of the difference in their chemical formulations."

in report prepared for test methods for elastomeric bearings on bridges [26]. This case can be explained by differences between manufacturing processes. Rubber production is a delicate process that can be easily affected by some other things. For example, not only chemicals used during production but also a little difference in temperature increase or pressure during vulcanization process also affect the quality of rubber. For this reason, standards provided by manufacturer are important.

Moreover, it can be seen in Figure 5.3 and again Table 5.1-3, damping ratio increases under 1 MPa tensile stress. As explained before, the reason of this is the decrease in stiffness associated with Mullins effect.

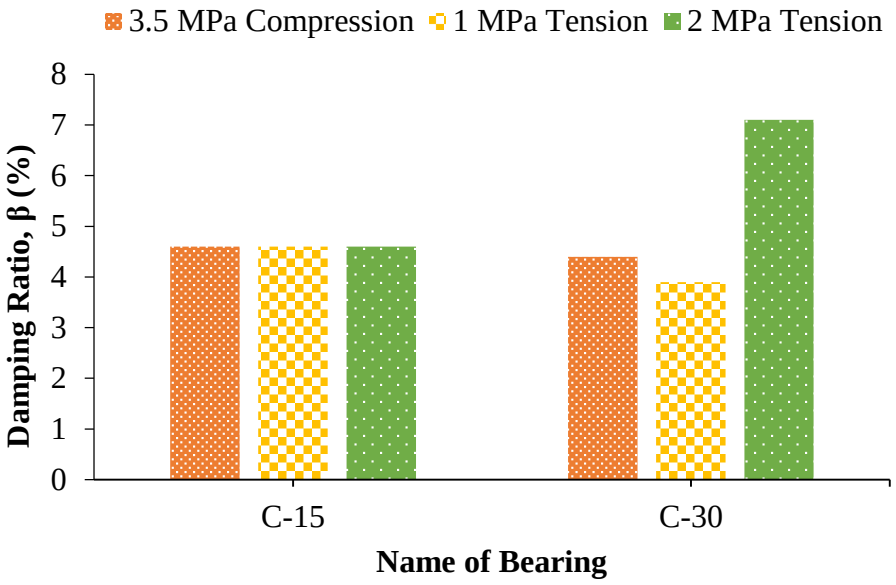

Figure 5.4: Comparison of percentage of damping of bearings under -3.5 MPa, 1 MPa and 2 MPa stress levels for concave edged bearings

Change in damping ratios of concave bearings is different. For C-15 bearing, damping ratio value is close to damping ratio of standard bearing having same size (O-15). However, its variation with tensile stress is too different. It can be seen in Figure 5.4 that damping ratio does not change with tension. According to this result, decrease in shear modulus of concave edged bearing is related to strain amplitude. For C-30 bearing, there seems to be a slight difference between damping ratio values. Yet, further research is suggested for a better understanding of the cause.

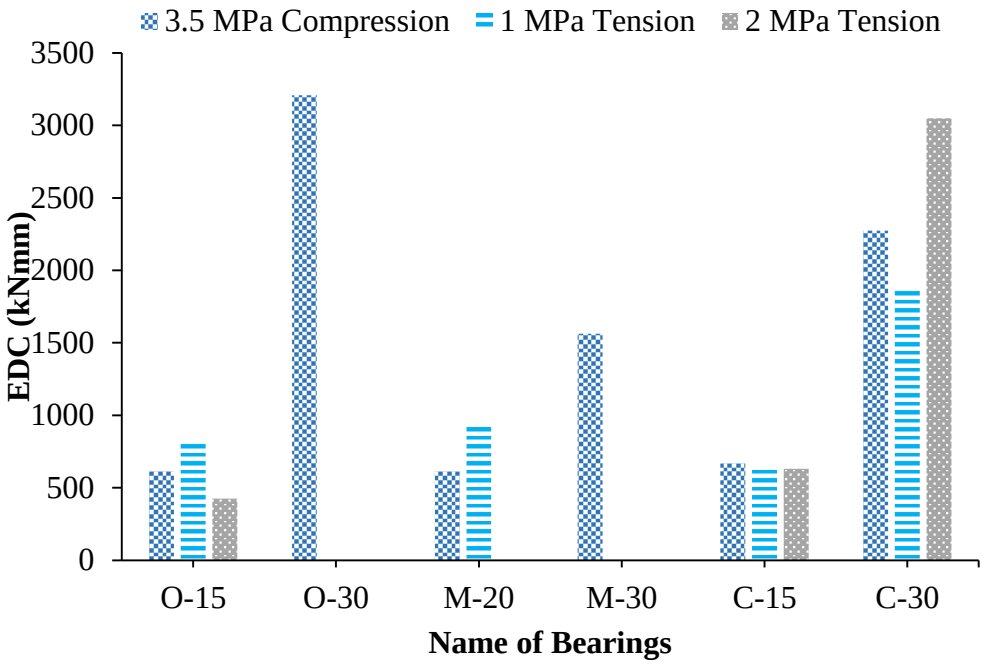

Figure 5.5: Comparison of EDC values of bearings under -3.5 MPa, 1 MPa and 2 MPa stress levels

O-30, M-30 and C-30 bearings have higher EDC values as depicted in Figures 5.5. In other word, difference in energy dissipation capabilities of bearings can be explained with the size effect. Besides, it can be seen that change in energy dissipation capacities is similar to damping ratio for all bearings.

Table 5.1: Summary shear modulus, damping ratio and EDC values at 3.5 MPa compression

Bearing Type	Shear Modulus		β_{eq} (%)	EDC (kNmm)
	TS EN 1337-3	BS 5400		
O-15	0.49	0.41	5	613
O-30	0.56	0.39	8.4	3208
M-20	0.82	0.91	3.4	613
M-30	0.71	0.87	2.7	1562
C-15	0.88	0.93	4.6	668
C-30	0.63	0.63	4.4	2273

Table 5.2: Summary of shear modulus, damping ratio and EDC values at 1 MPa tension

Bearing Type	Shear Modulus		β_{eq} (%)	EDC (kNmm)
	TS EN 1337-3	BS 5400		
O-15	0.27	0.26	6.6	826
O-30	-	-	-	-
M-20	0.76	0.78	6.7	922
M-30	-	-	-	-
C-15	0.85	0.86	4.6	628
C-30	0.59	0.66	3.9	1874

Table 5.3: Summary of shear modulus, damping ratio and EDC values at 2 MPa tension

Bearing Type	Shear Modulus		β_{eq} (%)	EDC (kNmm)
	TS EN 1337-3	BS 5400		
O-15	0.25	0.22	3.1	425
O-30	-	-	-	-
M-20	-	-	-	-
M-30	-	-	-	-
C-15	0.82	0.82	4.6	631
C-30	0.52	0.71	7.1	3049

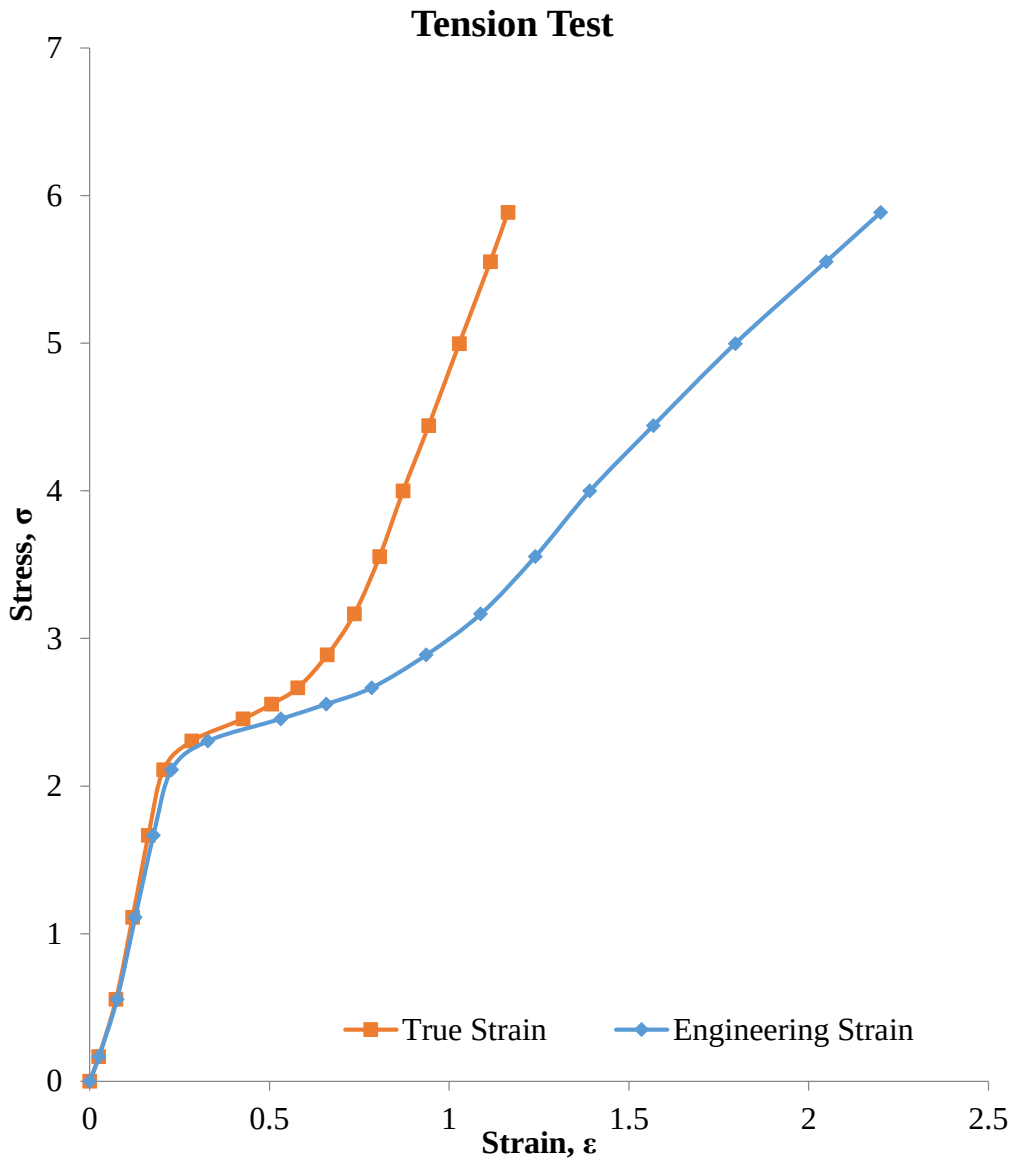

Figure 5.6: The typical relation curve of tensile stress-strain for O-15 bearing

In this part of test, O-15 and O-30 bearings are subjected to pure tension (without lateral displacement) and tensile stress is increased until the rubber gets ruptured. However, reliable data is obtained from O-15 bearing only. Photographs taken during pure tension test (stage by stage) of O-15 bearing is given in Appendix C with Figure C.6-12.

As indicated before at chapter 3, pure tension test of O-30 bearing failed because of bending of outer plates before rubber splitting. Besides, in report prepared for test methods for elastomeric bearings on bridges, failure types are divided into two categories as splitting failure in rubber and bond failure at interface between steel and elastomer [26]. It was also explained in chapter 4 that cyclic tension tests of M-20 and M-30 bearing failed because of cold bonding type of failure. Although there are some real-life applications, it was observed that cold bonding is not as effective as vulcanization process.

The reason behind this is explained in the following pages. At the end of experiment, obtained stress-strain curve is shown in Figure 5.5. As seen, both true and engineering strain is represented. Engineering strain is the simplest and most general measure of strain. However, it used to express small strain values since engineering materials like metals and concrete have small deformation. Another type of strain is true also called as logarithmic strain. These two strains are close to each other at small values but the start to differ at larger deformation. Using true strain may be more appropriate since it is additive which means that the summation of numerous differential segments [27]. According to stress-strain curve, there is a yield point which is a rubber property. When tensile stress approaches 2.1 MPa, the isolator will yield. After yield point reached, bearing starts to produce nonlinear deformation. 2.1 MPa is an acceptable value since it was reported that maximum tensile stress was 2.2 MPa during shaking table tests conducted by Feng et al.[5]. In addtion to these, maximum tensile stress level is recorded as 6 MPa till O-15 bearing rupture.

According to results, it is obvious that there are some uncertainties about bearing behavior under tension. It is not only related to variable properties of rubber but also some unpredictable deformation of joint parts. While tensile deformation of bearing is tested, the deformation of joint plates and joint bolts should also be considered in order to comprehend accurate bearing behavior. Study conducted by Hara et al. showed that flange plate deformation slightly affects tension and shear property of bearing [28]. However, this effect might be significant considering that it is related to bending stiffness of flange plates and magnitude of tensile stress.

CHAPTER 6

SUMMARY OF CONCLUSIONS

6.1. Summary of Conclusions

Consequently, it can be said that seismic isolation performance of standard circular type RBs under tensile stress is acceptable up to 2 MPa. As known, tensile stress level is generalized up to 2 MPa for all type and shape bearings in Japan and this study reveals supportive results for standard steel reinforced elastomeric bearings. It means that structure design is possible without considering a lockup system which causes additional cost in construction. Nevertheless, there should be carried out more experiments that consider the difference of shape factor and different types of bearings.

Moreover, promising results are obtained from tests conducted via new type of bearing having concave shape at the edges. Stability of damping ratio under tensile force is significant. It opens the door to new fields of study with this new feature.

Finally, it should be reminded that this thesis is a preliminary work for further researches and in the following part there are some suggestions that can be considered for future studies.

6.2. Recommendations for Future Researches

For future studies, following recommendations are suggested;

- Testing different type of RBs (like, BRB, LRB and HRB) can be suggested.
- RBs in different shape factors may be tested.
- Square and rectangular RBs may be tested.
- Effect of temperatures on tension characteristics may be investigated.
- Behavior of bearing after yield point can be investigated.

A new test schedule can be prepared for concave edged bearings;

- Its behavior under compression, tension and shear stresses may be examined in a more detailed way.
- Limit characteristics may be determined.
- Effect of shape factor on concave type bearing can be investigated.
- It can be produced with central hole and tested with different filler types.
- Analytical model may be established

REFERENCES

[1] B. Y. Moon, G. J. Kang, B. S. Kang, G. S. Kim, and J. M. Kelly, "Mechanical Properties of Seismic Isolation System with Fiber-Reinforced Bearing of Strip Type," *International Applied Mechanics,* vol. 39, pp. 1231-1239, 2003.

[2] I. G. Buckle and R. L. Mayes, "Seismic isolation: History, application and performance - A world view," *Earthquake Spectra*, vol. 6, pp. 161-201, 1990.

[3] F. Naeim and J. M. Kelly, *Design of seismic isolated structures*. Canada: John Wiley & Sons, Inc., 1999.

[4] I. Mangerig and T. Mano, "Characteristics of various elastomeric bearings in tension," *Steel Construction,* vol. 2, pp. 161-166, 2009.

[5] D. Feng, T. Miyami, X. Lu, and I. Masayoshi, "A shaking table test study on shear tensile properties of lead rubber bearings," presented at the 13th World Conference on Earthquake Engineering, Vancouver, B.C., Canada, 2004.

[6] California Department of Transportation (Caltrans). *Bridge Design Specifications, Section 14*, 2000

[7] American Association of State Highway and Transportation Officials (ASSHTO). *Load Resistant Factor Design (LFRD) Bridge Design Specification, 5th Edition*, 2010

[8] American Society of Civil Engineers (ASCE). *Minimum Design Loads for Buildings and Other Structures,* SEI 7-10, 2010

[9] European Committee For Standardization (European Standard). *EN 15129: Anti-seismic devices, Section ,* 2009

[10] R. S. Jangid and T. K. Datta, "Seismic behaviour of base-isolated buildings: a state-of-the-art review," in *Proceeding of The Institution of Civil Engineers - Structures and Buildings*, 1995, pp. 186-203.

[11] K. Takabayashi, K. Mizukoshi, A. Yasaka, and M. Iızuka, "Failure test of laminated rubber bearings with various shapes," presented at the Earthquake Engineering, 10th World Conference Balkema, Rotterdam, 1992.

[12] J. M. Kelly, "Seismic isolation systems for developing countries," *Earthquake Spectra*, vol. 18, pp. 385-406, Aug 2002.

[13] C. Ozkaya, U. Akyuz, A. Caner, M. Dicleli, and S. Pinarbasi, "Development of a new rubber seismic isolator: 'Ball Rubber Bearing (BRB)'," *Earthquake Engineering & Structural Dynamics*, vol. 40, pp. 1337-1352, Oct 2011.

[14] A. Turer and B. Ozden, "Seismic base isolation using low-cost Scrap Tire Pads (STP)," *Materials and Structures*, vol. 41, pp. 891-908, Jun 2008.

[15] E. Takaoka, Y. Takenaka & A. Nimura, "Shaking table test and analysis method on ultimate behavior of slender base-isolated structure supported by laminated rubber bearings" *Earthquake Engineering and Structural Dynamics*, vol. 40, pp. 551-570, Aug 2010.

[16] R. Maseki, I. Nagashima, and M. Hisano, "An experimental study on application of hybrid-type base isolation system to high-rise buildings," in *Proceedings of 12th World Conference on Earthquake Engineering*, Auckland, New Zealand, 2000, p. 1875.

[17] N. Iwabe, M. Takayama, N. Kani, and A. Wada, "Experimental study on the effect of tension for rubber bearings," in *12th World Conference on Earthquake Engineering*, 2000, p. 1290.

[18] Q. Yang, W. Liu, W. He, and D. Feng, "Tensile Stiffness and Deformation Model of Rubber Isolators in Tension and Tension-Shear States," *Journal of Engineering Mechanics*, vol. 136, pp. 429-437, 2010.

[19] A. Dorfmann, "Stress softening of elastomers in hydrostatic tension," *Acta Mechanica*, vol. 165, pp. 117-137, Nov 2003.

[20] M. C. Griffith, I. D. Aiken, and J. M. Kelly, "Dısplacement control and uplıft restraınt for base-ısolated structures," *Journal of Structural Engineering-Asce*, vol. 116, pp. 1135-1148, Apr 1990.

[21] American Association of State Highway and Transportation Officials (ASSHTO). *Load Resistant Factor Design (LFRD) Bridge Design Specification, 3rd Edition*, 2005

[22] I. Buckle, M. C. Constantinou, M. Dicleli & H. Ghasemi, *"Seismic Isolation of Highway Bridges"*. Special Report MCEER-06-SP07, 2006.

[23] AASHTO M 251-06. *Standard Specification for Plain and Laminated Elastomeric Bridge Bearings*, 2006

[24] M. Rahim and A. M. Kamarudin, "On the variation of the experimental shear modulus of elastomers," *9th National Symposium on Polymeric Materials (Nspm 2009)*, vol. 11, p. 5, 2010.

[25] A. Dorfmann and S. Burtscher, "Aspects of Cavitation Damage in Seismic Bearings," *Journal of Structural Engineering*, vol. 126, pp. 573-579, 2000.

[26] Y. J. Arditzoglou, J. A. Yura, and A. H. Haines, "Test methods for elastomeric bearings on bridges," Center for Transportation Research The University of Texas at Austin FHWA-TX-96/1304-2, 1995.

[27] P. Kelly, Lecture Notes in Solid Mechanics Part I: An Introduction to Solid Mechanics,http://homepages.engineering.auckland.ac.nz/~pkel015/SolidMechanicsBooks/index.html, last visited on August 2014

[28] K. Fukayawa, T. Hara, M. M., M. Tachibana, and J. Tajima, "Experimental Study on Tensile Performance and Shearing Performance under Tensile Force of High Damping Rubber Bearings Part 1 to 3," in *Annual Meeting Architectural Institute of Japan*, 1998, pp. 1137–1142.

APPENDIX A

EXPERIMENTAL HYSTERESIS LOOPS

In Appendix A part, experimental hysteresis loops are presented for all tests. There are no corrections on hysteresis loops. In other words, they are original.

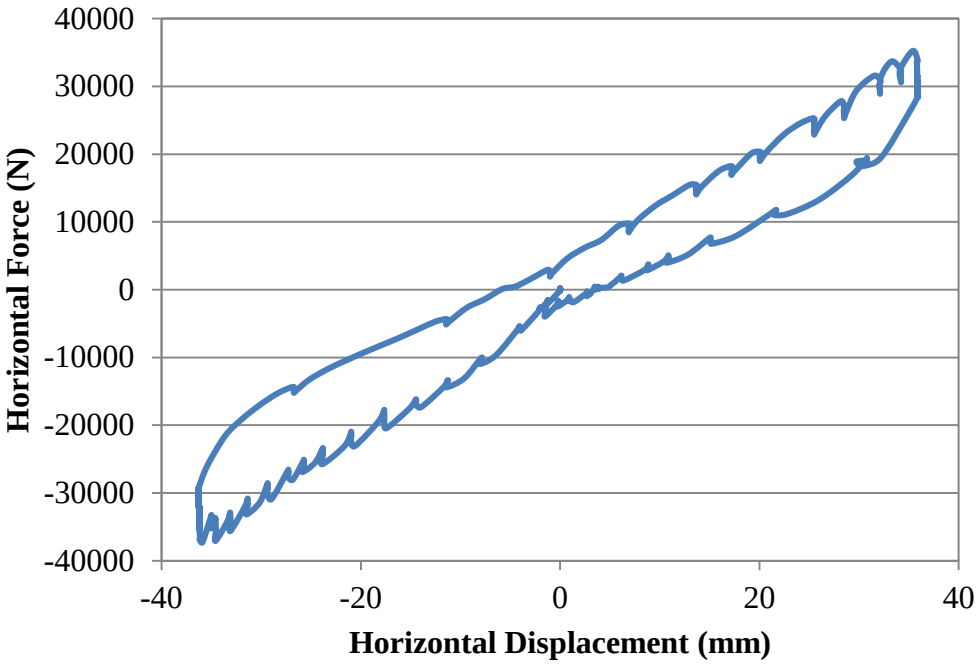

Figure A.1: Hysteresis loop of O-15 pre-conditioning test under 3.5 MPa compression

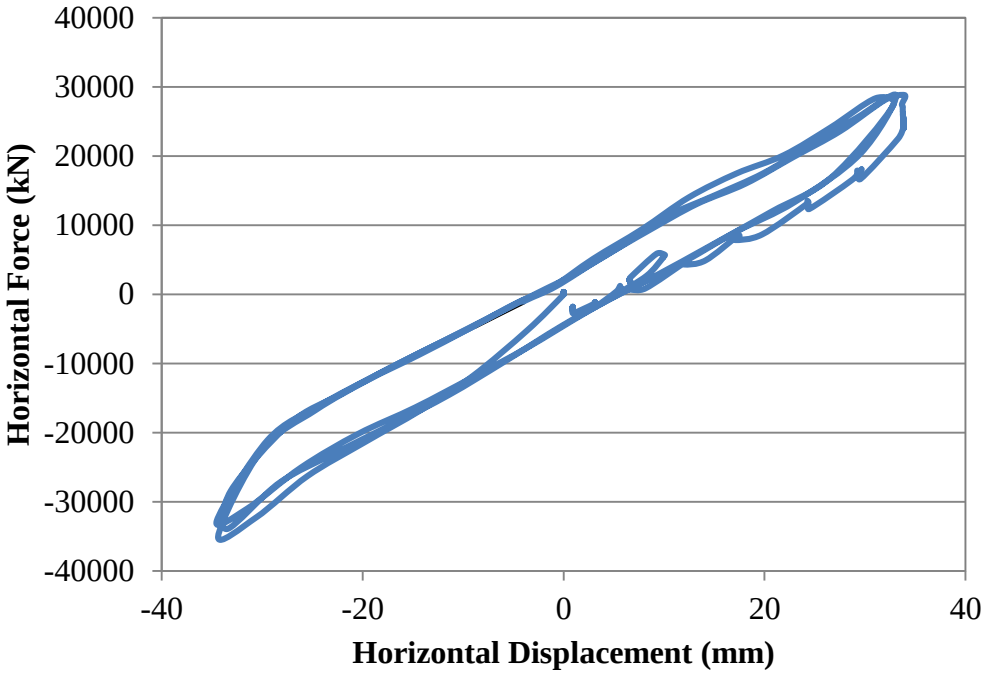

Figure A.2: Hysteresis loop of O-15 cyclic test under 3.5 MPa compression

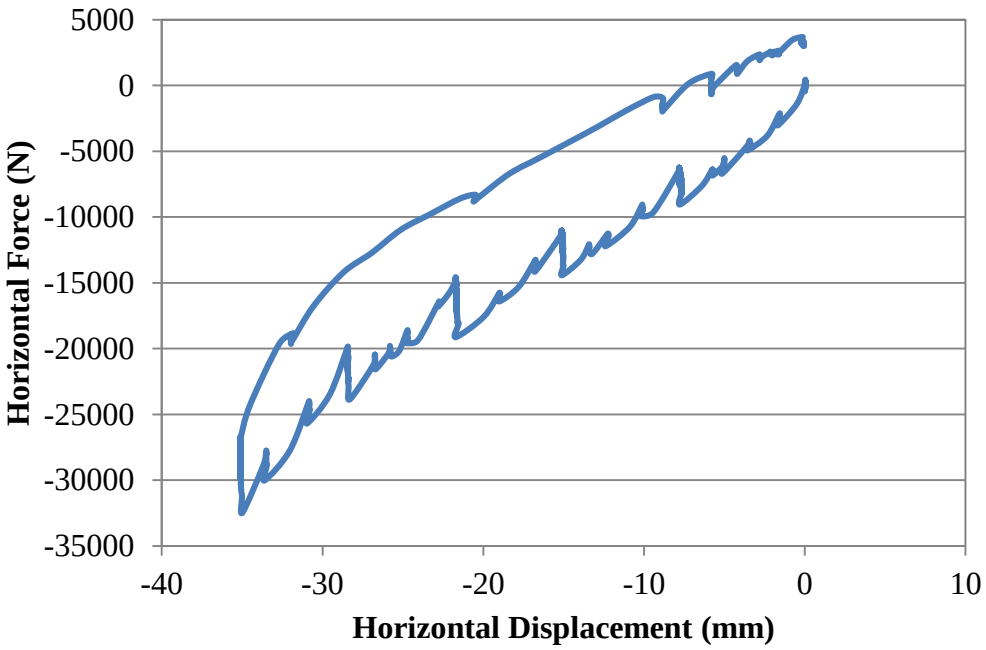

Figure A.3: Hysteresis loop of O-15 staged test under 3.5 MPa compression

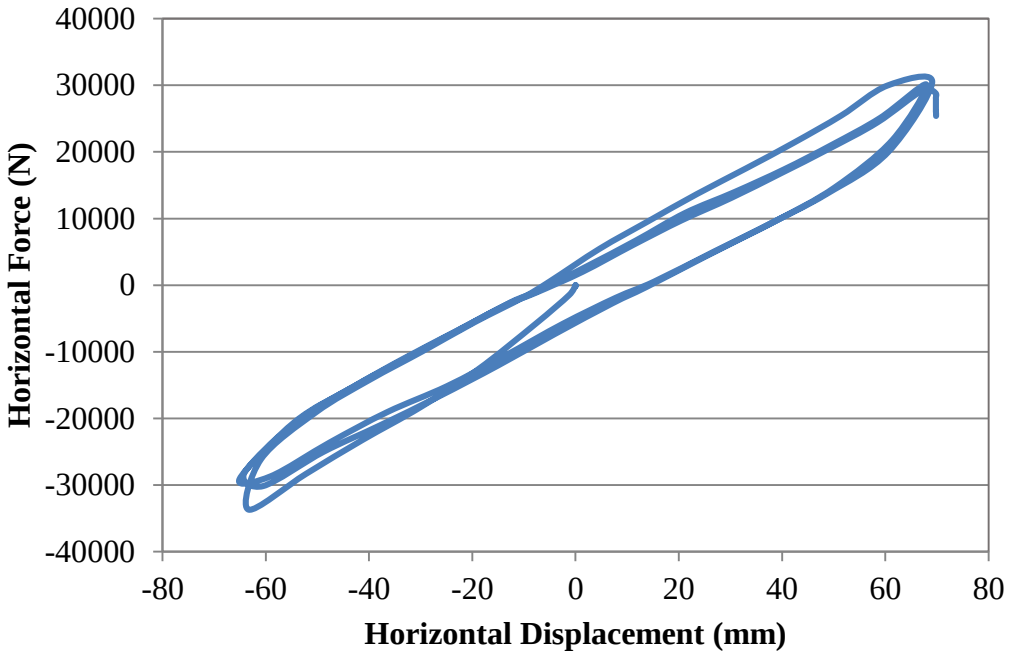

Figure A.4: Hysteresis loop of O-15 cyclic test under 1 MPa tension

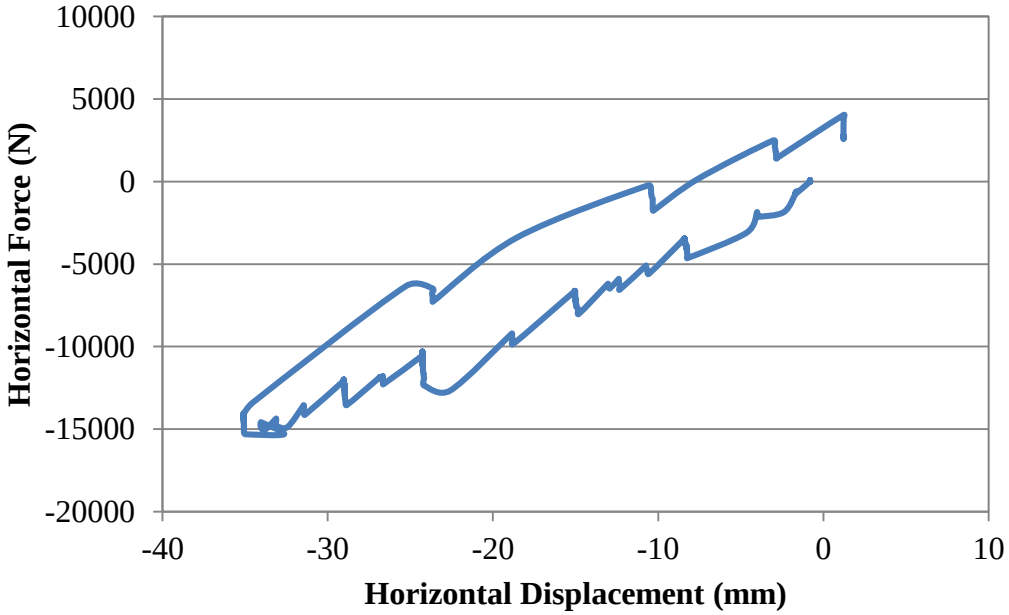

Figure A.5: Hysteresis loop of O-15 staged test under 1 MPa tension

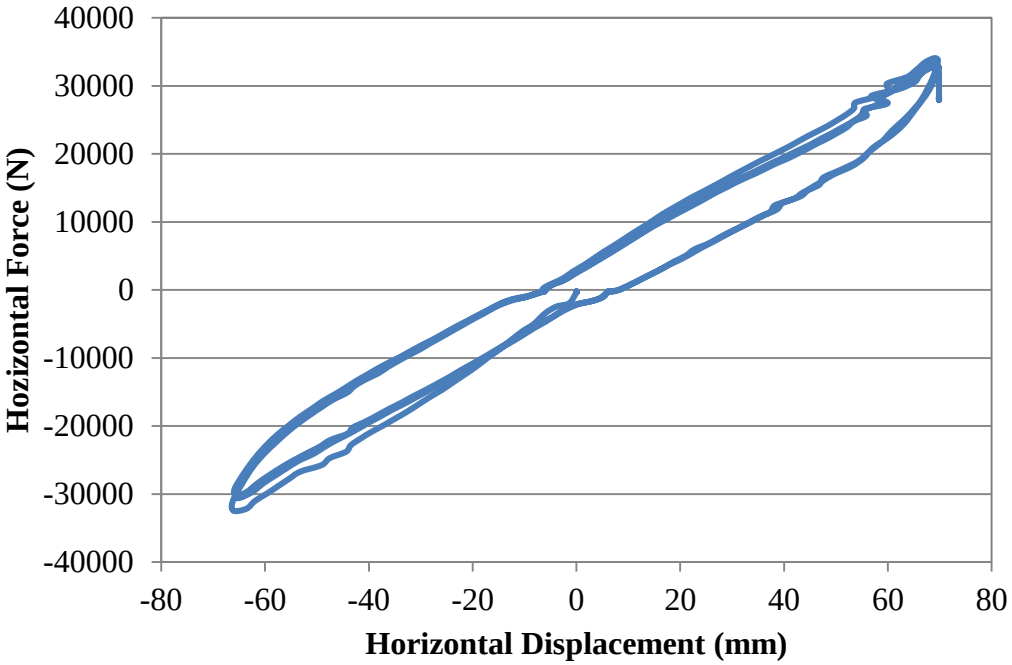

Figure A.6: Hysteresis loop of O-15 cyclic test under 2 MPa tension

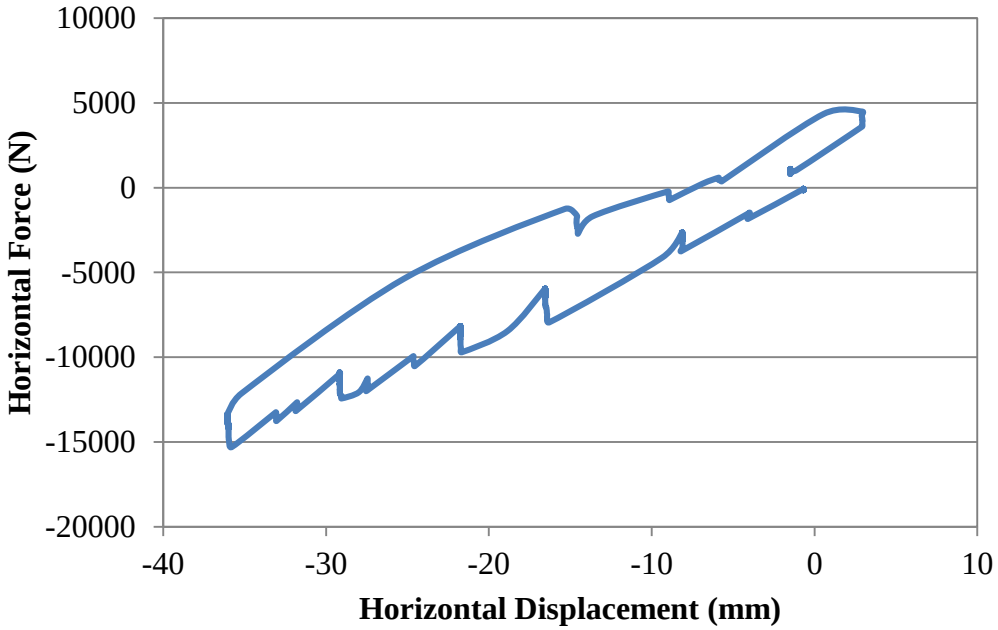

Figure A.7: Hysteresis loop of O-15 staged test under 2 MPa tension

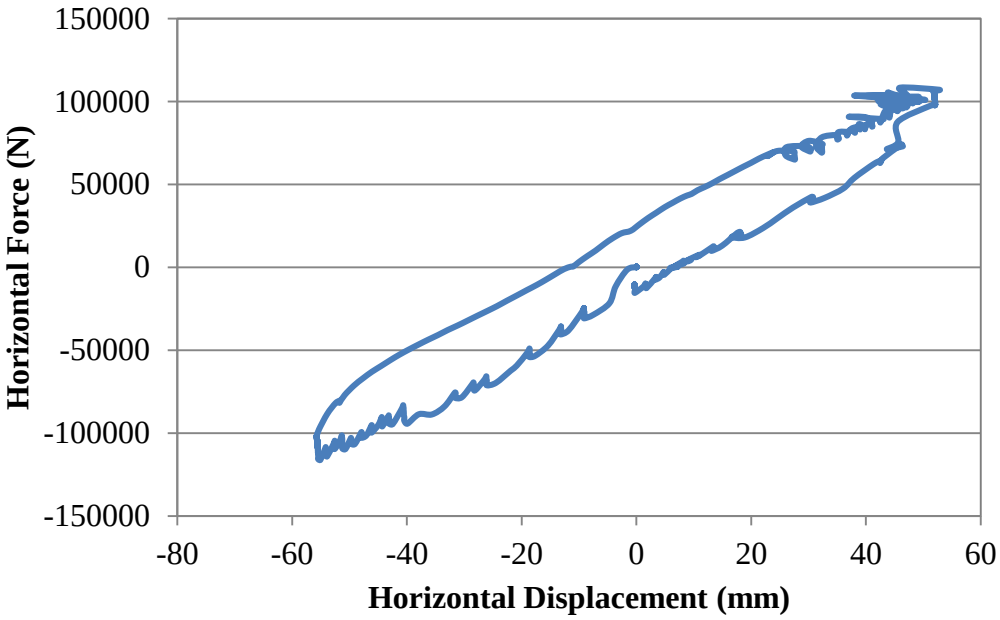

Figure A.8: Hysteresis loop of O-30 pre-conditioning test under 3.5 MPa compression

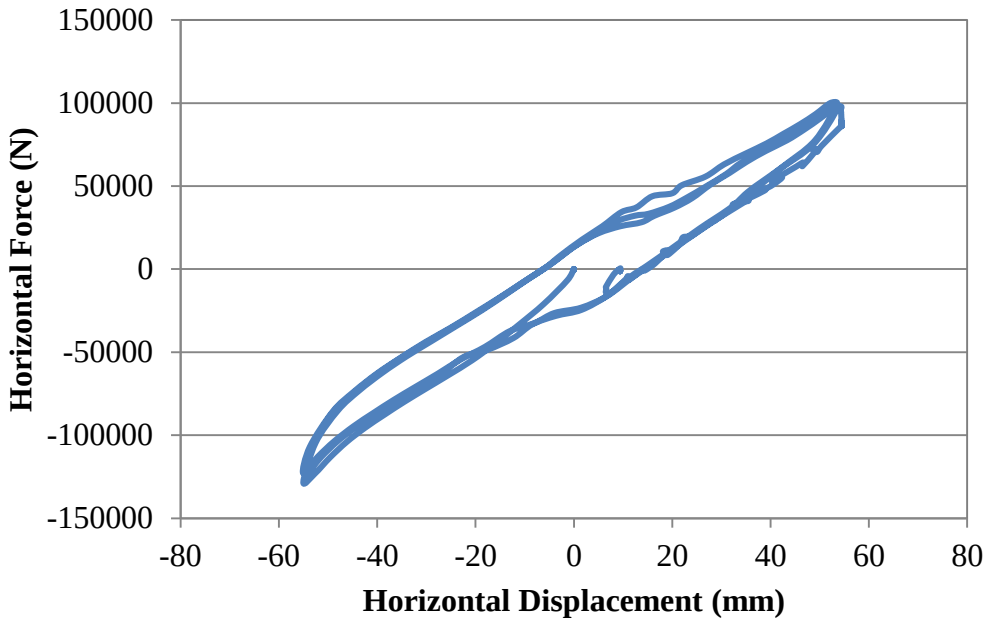

Figure A.9: Hysteresis loop of O-30 cyclic test under 3.5 MPa compression

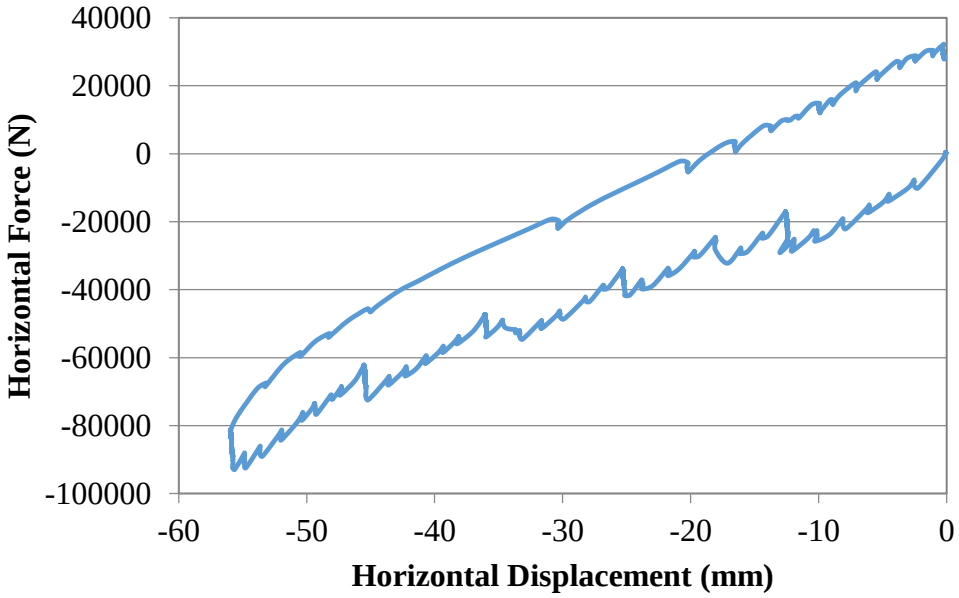

Figure A.10: Hysteresis loop of O-30 staged test under 3.5 MPa compression

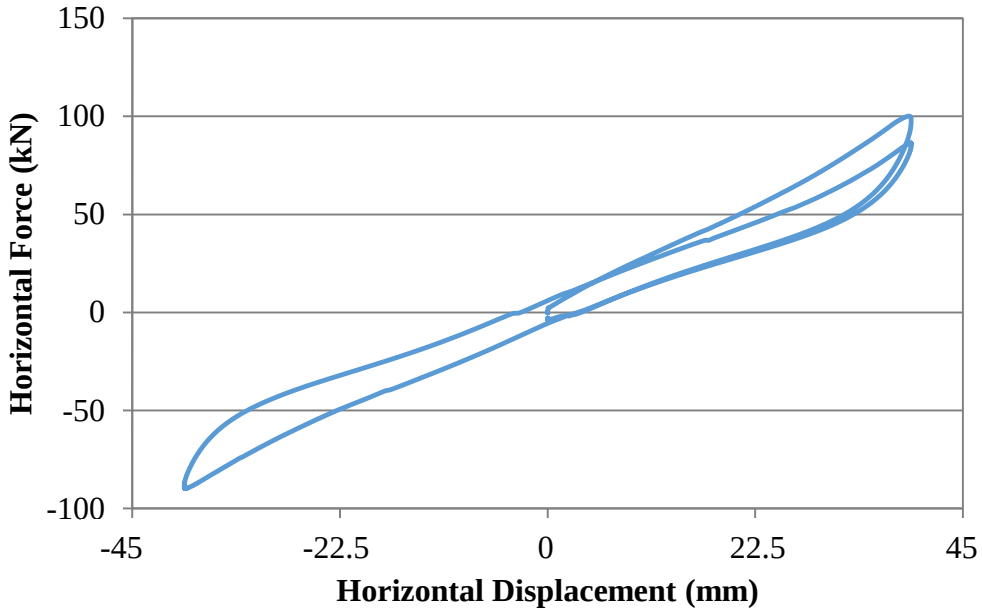

Figure A.11: Hysteresis loop of M-20 pre-conditioning test under 3.5 MPa compression

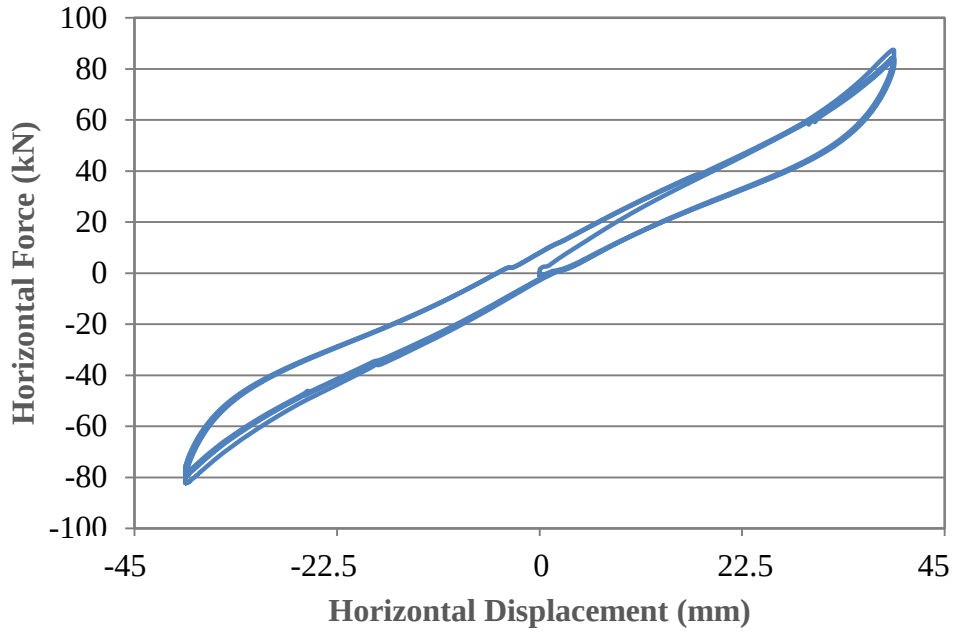

Figure A.12: Hysteresis loop of M-20 cyclic test under 3.5 MPa compression

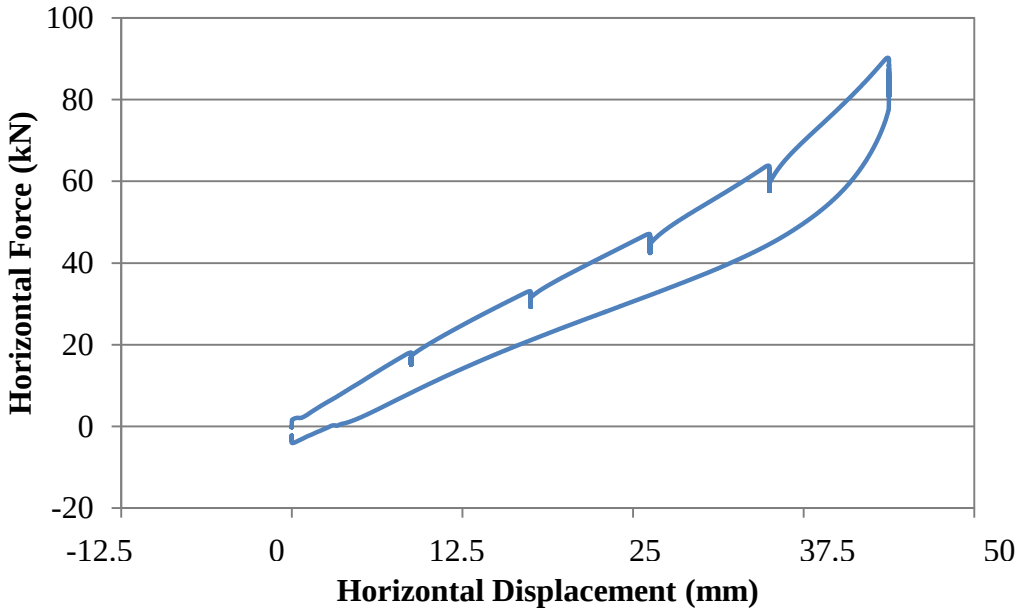

Figure A.13: Hysteresis loop of M-20 staged test under 3.5 MPa compression

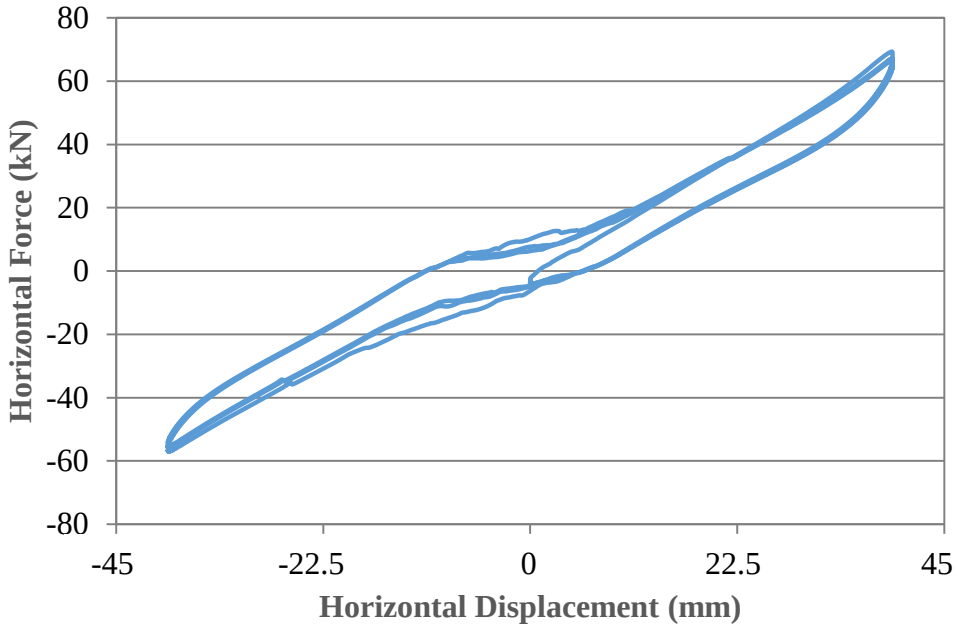

Figure A.14: Hysteresis loop of M-20 cyclic test under 1 MPa tension

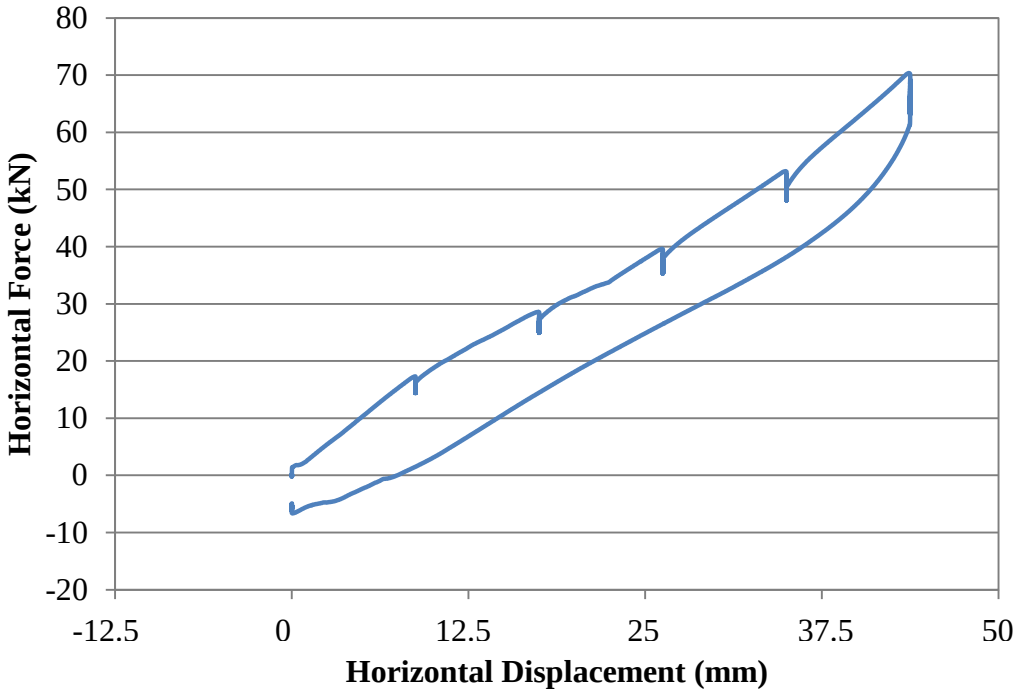

Figure A.15: Hysteresis loop of M-20 staged test under 1 MPa tension

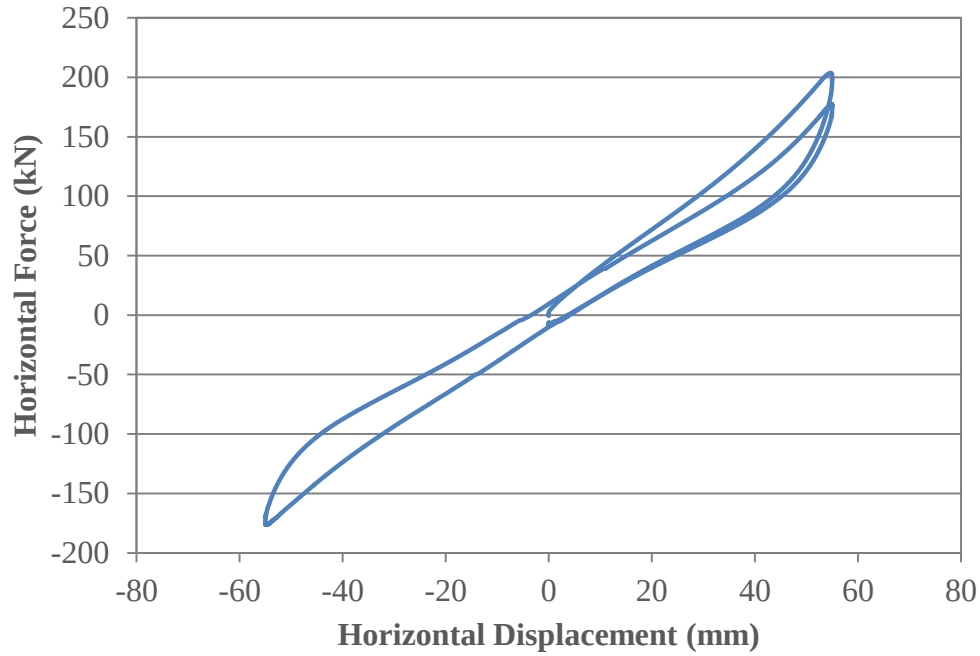

Figure A.16: Hysteresis loop of M-30 pre-conditioning test under 3.5 MPa compression

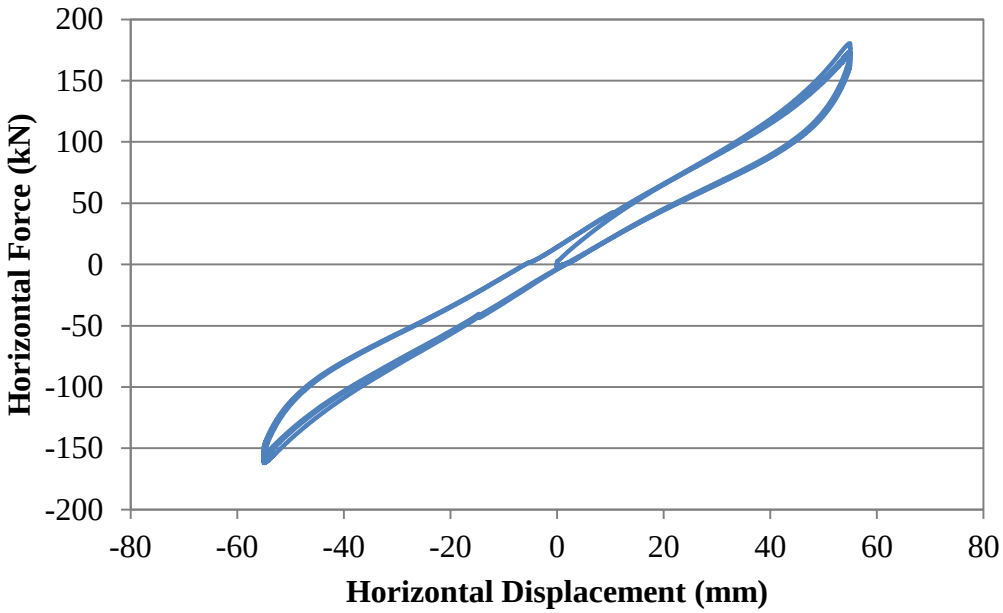

Figure A.17: Hysteresis loop of M-30 cyclic test under 3.5 MPa compression

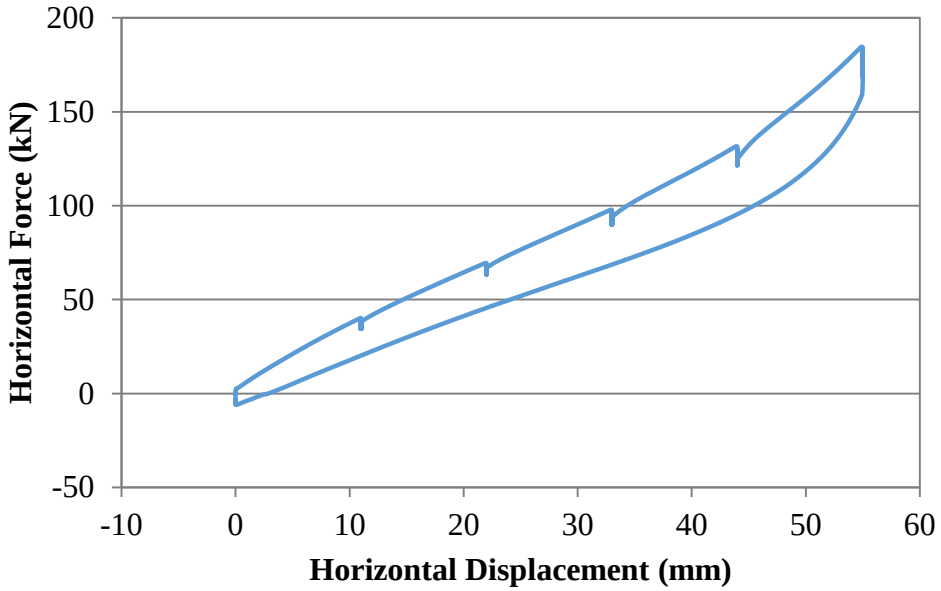

Figure A.18: Hysteresis loop of M-30 staged test under 3.5 MPa compression

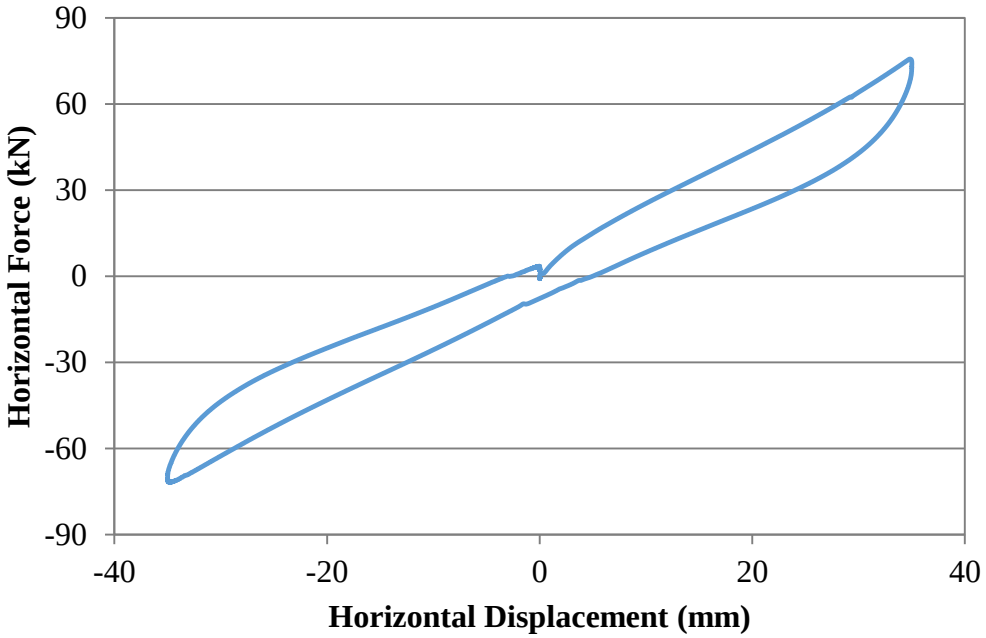

Figure A.19: Hysteresis loop of C-15 pre-conditioning test under 3.5 MPa compression

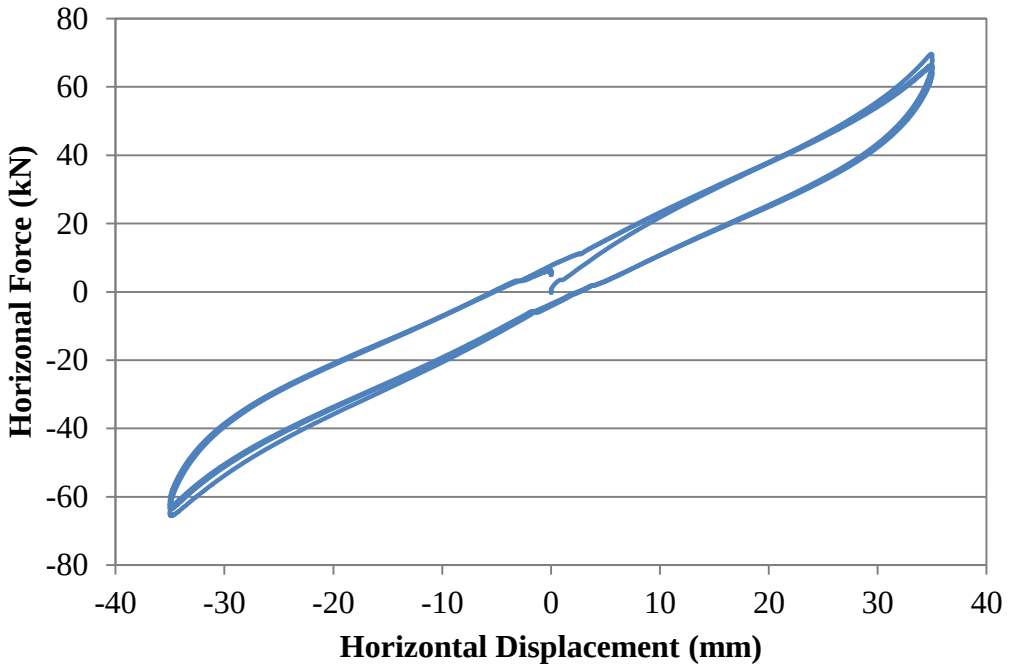

Figure A.20: Hysteresis loop of C-15 cyclic test under 3.5 MPa compression

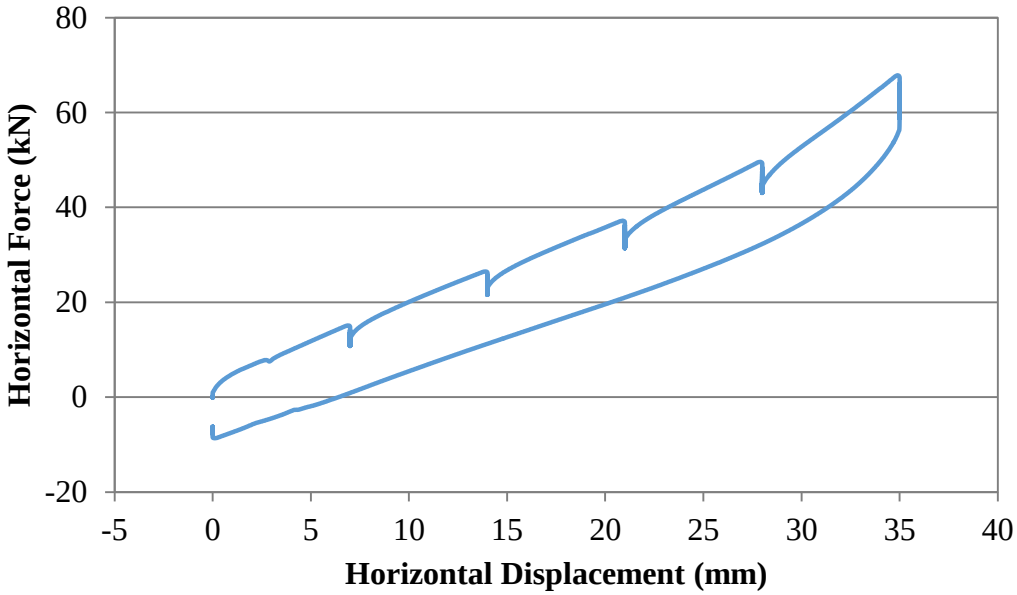

Figure A.21: Hysteresis loop of C-15 staged test under 3.5 MPa compression

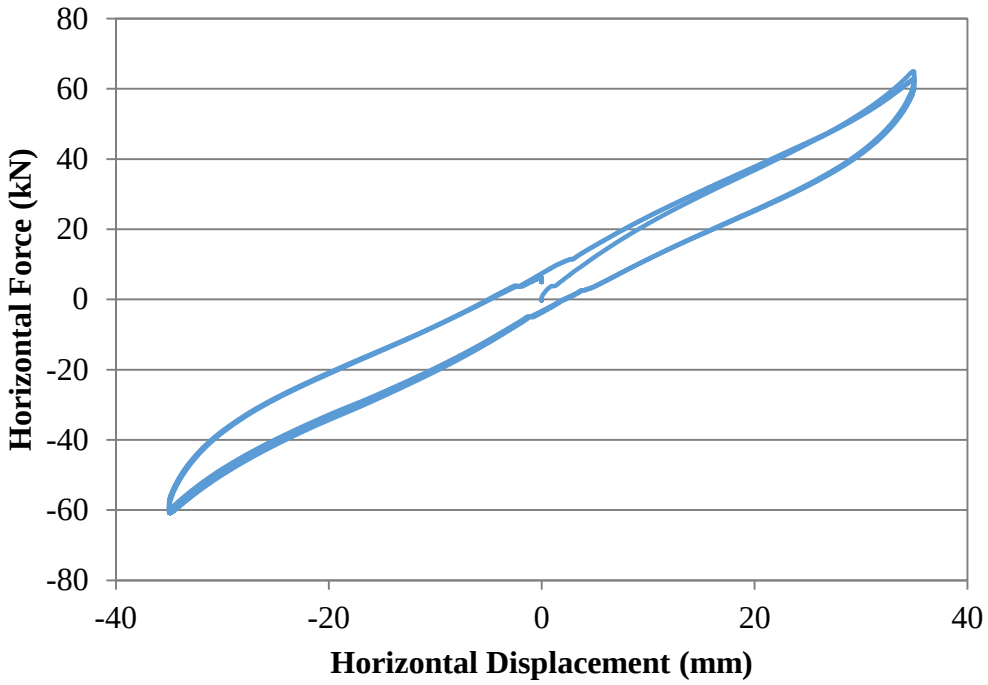

Figure A.22: Hysteresis loop of C-15 cyclic test under 1 MPa tension

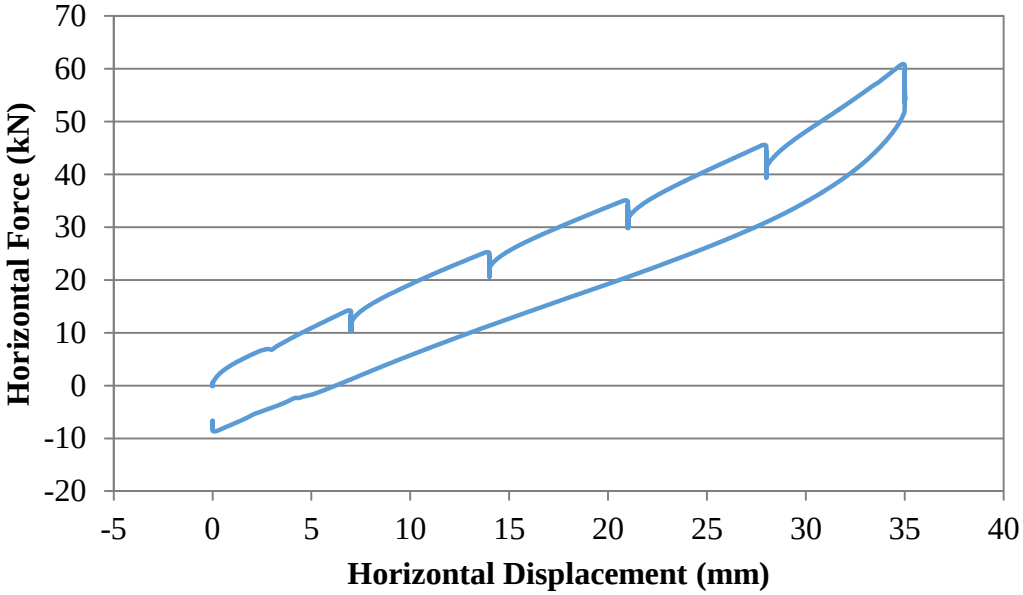

Figure A.23: Hysteresis loop of C-15 staged test under 1 MPa tension

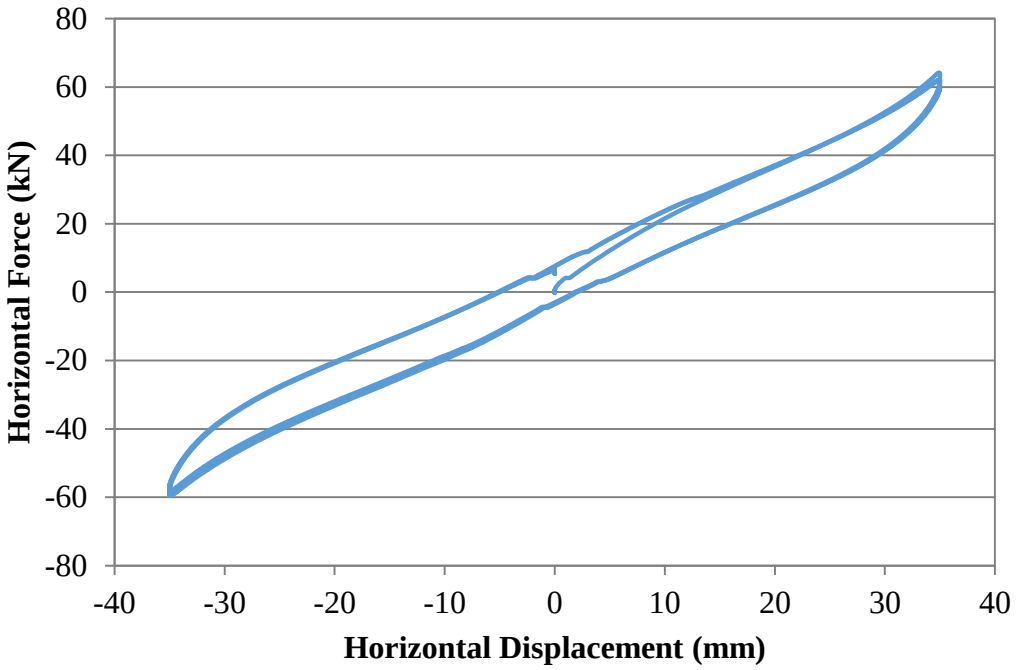

Figure A.24: Hysteresis loop of C-15 cyclic test under 2 MPa tension

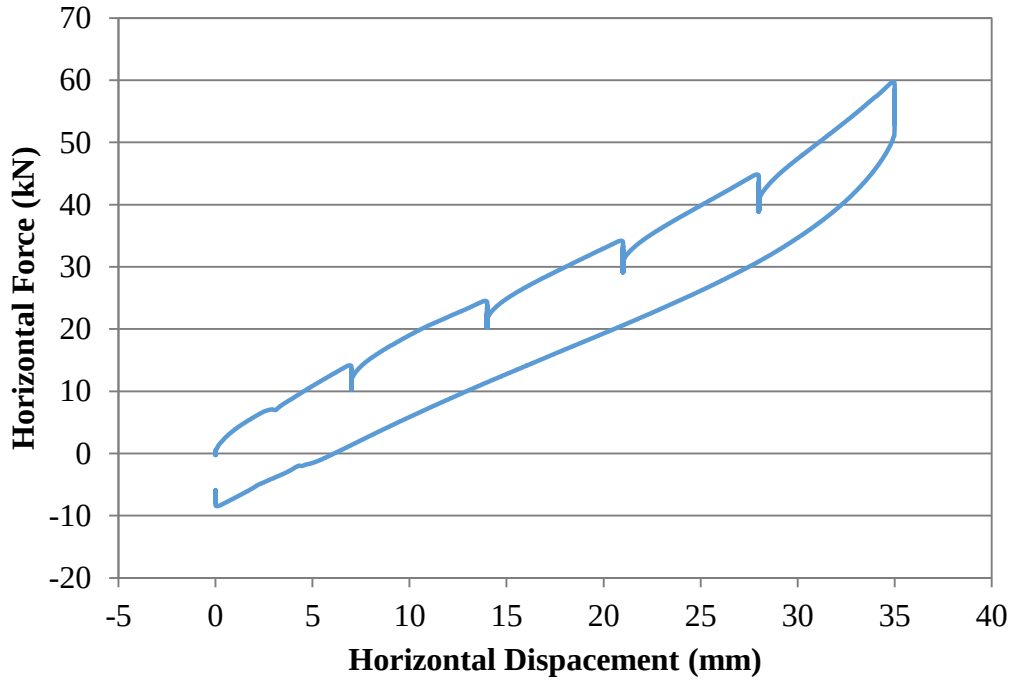

Figure A.25: Hysteresis loop of C-15 staged test under 2 MPa tension

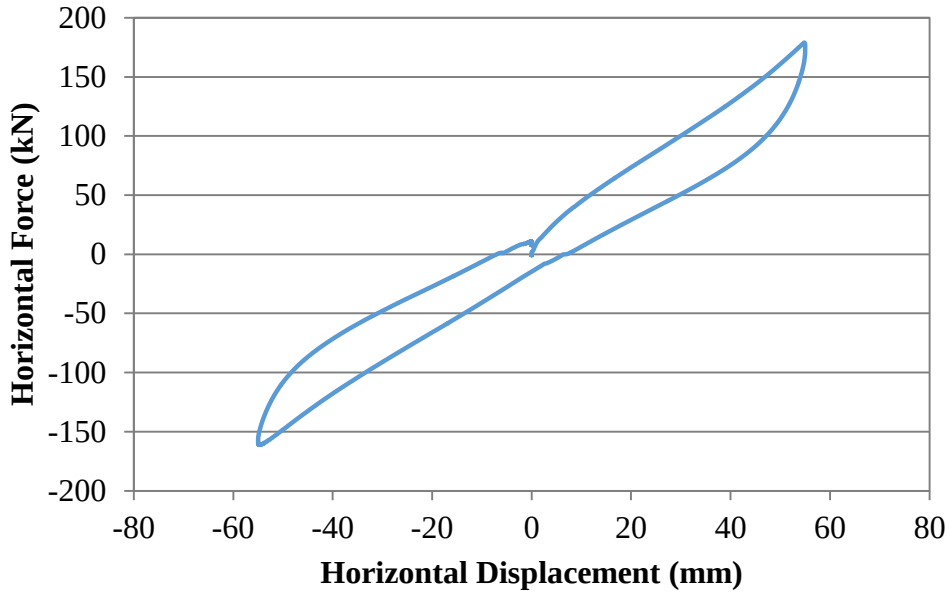

Figure A.26: Hysteresis loop of C-30 pre-conditioning test under 3.5 MPa compression

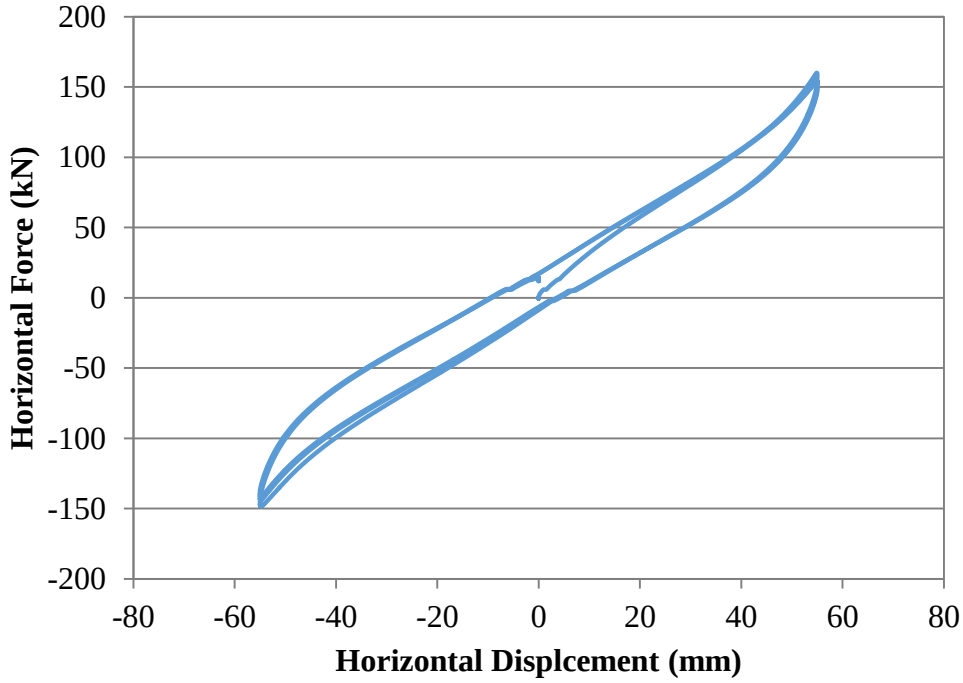

Figure A.27: Hysteresis loop of C-30 cyclic test under 3.5 MPa compression

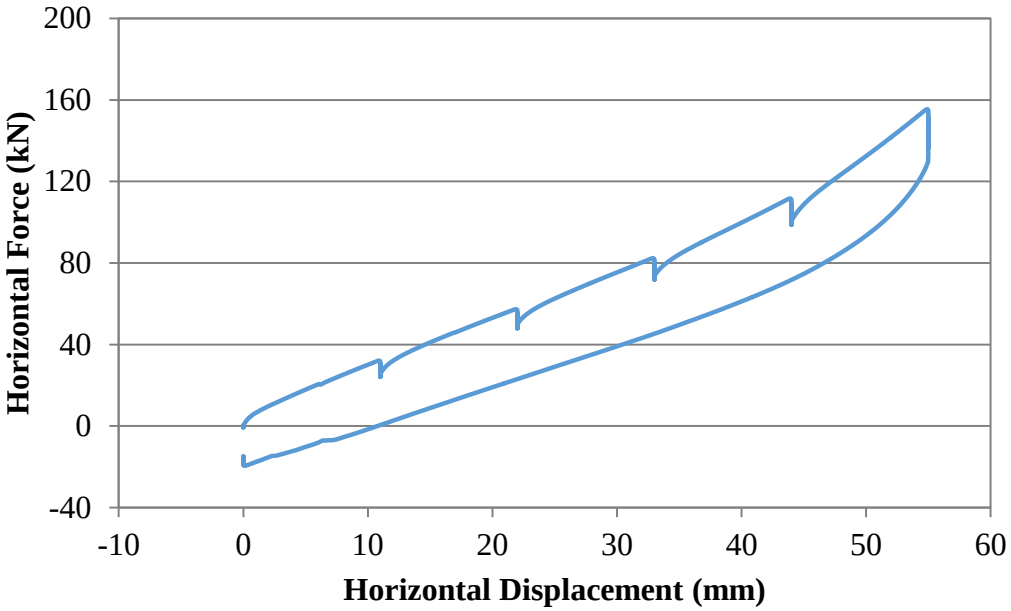

Figure A.28: Hysteresis loop of C-30 staged test under 3.5 MPa compression

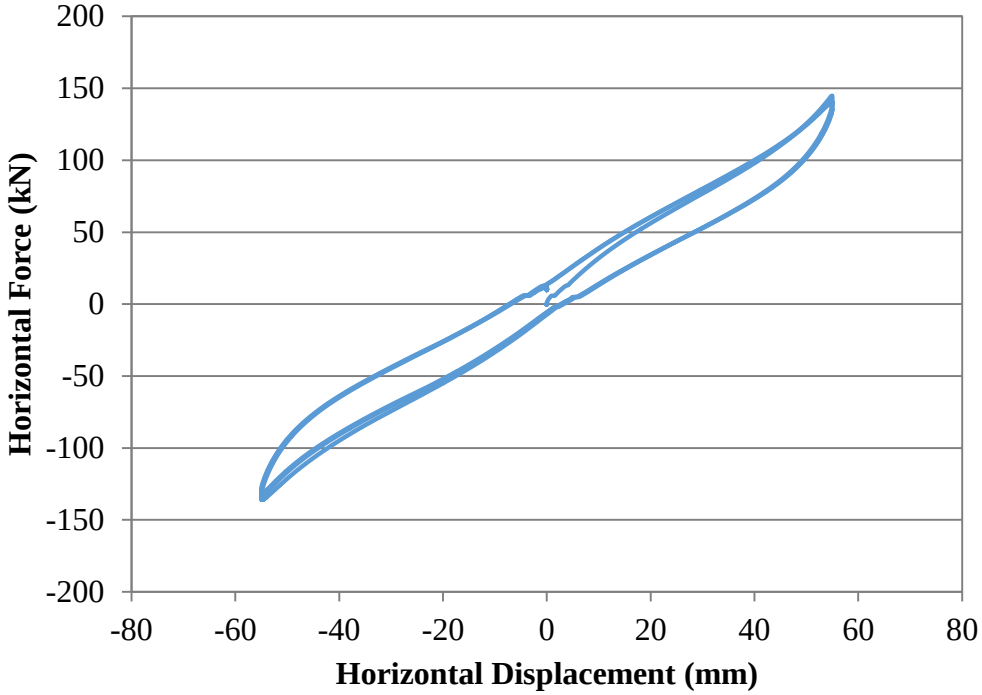

Figure A.29: Hysteresis loop of C-30 cyclic test under 1 MPa tension

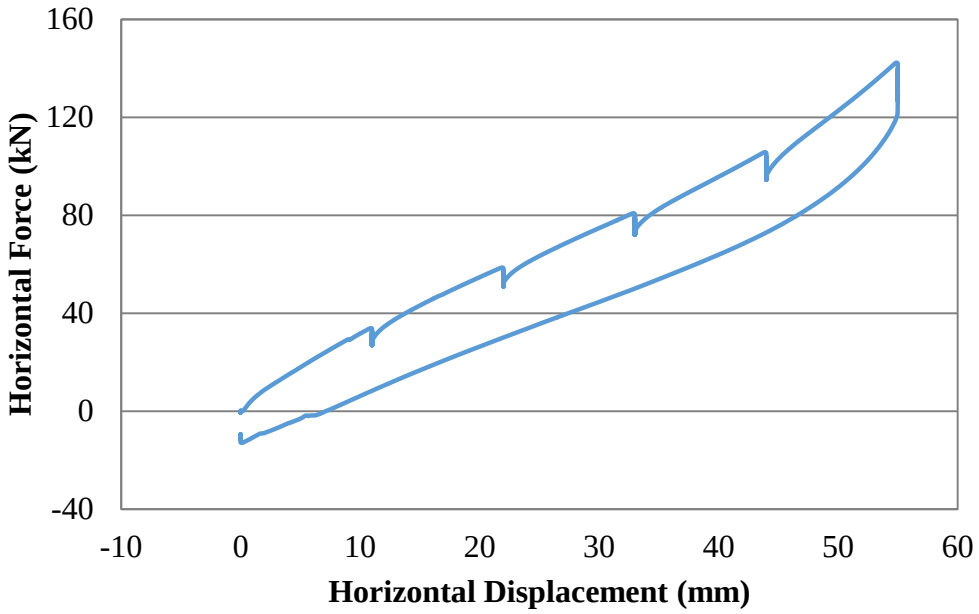

Figure A.30: Hysteresis loop of C-30 staged test under 1 MPa tension

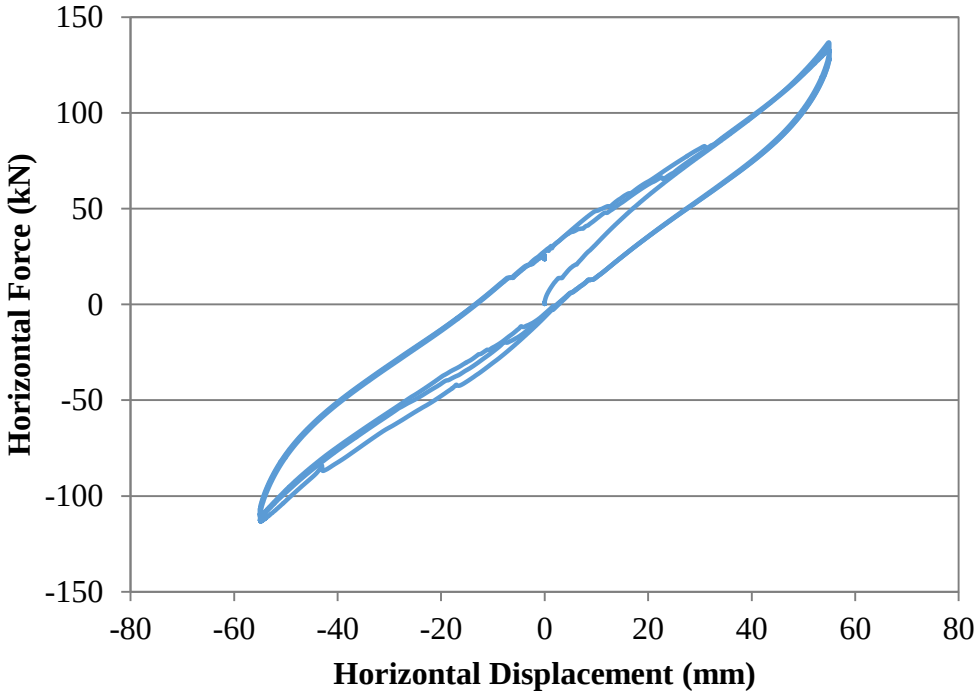

Figure A.31: Hysteresis loop of C-30 cyclic test under 2 MPa tension

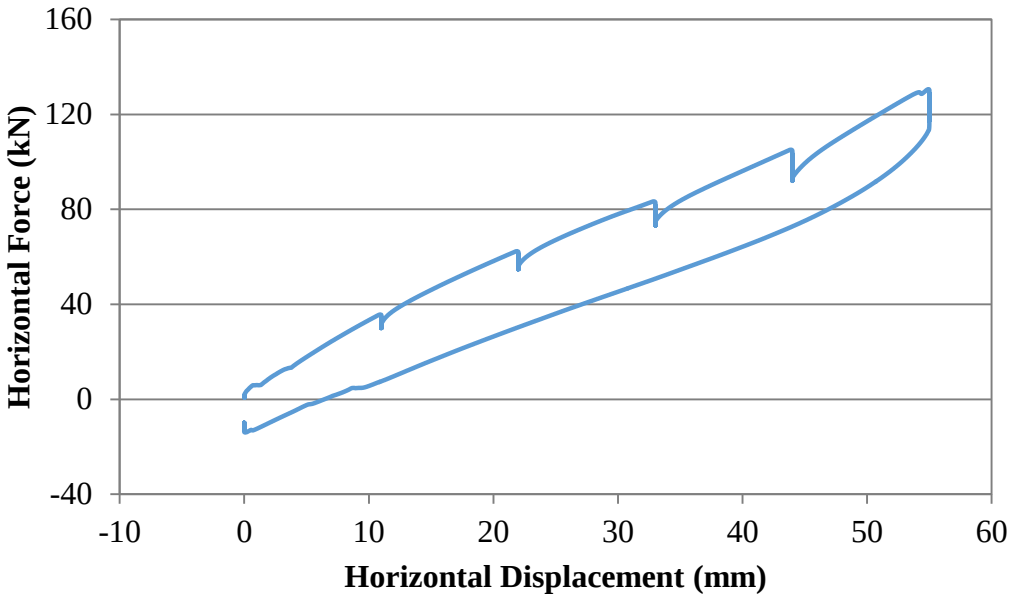

Figure A.32: Hysteresis loop of C-30 staged test under 2 MPa tension

APPENDIX B

SAMPLE CALCULATIONS

In Appendix B part, sample calculation for shear modulus and damping ratio is given. Calculations are done for only O-30 bearing. While shear modulus (BS 5400) value is calculated, force and displacement data is obtained from staged test. Determined values are listed in Table B.1. Moreover, damping ratio is calculated from fully reverse cyclic tests.

Shear modulus calculation with TS EN 1337-3

Shear stress is;

$$\tau_q = \frac{F_x}{A}$$ (TS EN 1337-3 Equation F.1)

$$\tau_1 = \frac{36221\ N}{\left(\frac{\pi(300\ mm)^2}{4}\right) x\ 2} = 0.256\ MPa$$

$$\tau_2 = \frac{80788\ N}{\left(\frac{\pi(300\ mm)^2}{4}\right)\ x\ 2} = 0.571\ MPa$$

Shear strain is;

$$\varepsilon_q = \frac{V_x}{T_q}$$ (TS EN 1337-3 Equation F.2)

$$\varepsilon_1 = \frac{12.5\ mm}{40\ mm} = 0.312$$

$$\varepsilon_2 = \frac{35\ mm}{40\ mm} = 0.875$$

Shear modulus is;

$$G = \frac{\tau_2 - \tau_1}{\varepsilon_2 - \varepsilon_1}$$ (TS EN 1337-3 Equation F.3)

$$G = \frac{0.571 - 0.256}{0.875 - 0.312} = 0.56\ MP$$

Shear modulus calculation with BS 5400

Shear modulus is;

$$G = \frac{K_s . T_q}{A}$$ (BS 5400 : Section 9.2 : 1983 Appendix A.4)

$$K_s = \frac{34335\ N}{25\ mm} = 1373.4\ N/mm$$

$$G = \frac{(1373.4\ N/mm)\ x\ (40\ mm)}{\left(\frac{\pi(300^2)}{4}\right) mm^2\ x\ 2} = 0.39\ MPa$$

Damping Ratio

Table B.1: Max. horizontal displacement, effective stiffness, characteristic strength and yield strain values for O-30 bearing

O-30 (300 mm ϕ)	max.	min.	average
d_{max}	55 mm	52 mm	53.5 mm
Q_d	24500 N	13243 N	18871.5 N
K_{eff}	2374.192 N/mm	1857.919 N/mm	2116.056 N/mm
d_y	-	-	11 mm

$$\beta = \frac{2\ Q_d\left(d_{max} - d_y\right)}{\pi\left(K_{eff} d_{max}^2\right)}$$ (AASHTO Guide Specifications for Seismic Isolation Design 1999: C7.1 Page 29)

$$\beta = \frac{2\ \left(\frac{18871.5}{2}\ N\right)(53.5\ mm - 11\ mm)}{\pi\left(\frac{2116.056}{2}\ N/mm\right)(53.5\ mm)^2} = 0.084$$

APPENDIX C

PHOTOGRAPHS

In Appendix C part, pictures which are taken during test are given.

Figure C.1: O-30 bearing in the case of an 100% shear deformation under tension

Figure C.2: O-15 bearing in the case of an100% shear deformation under tension

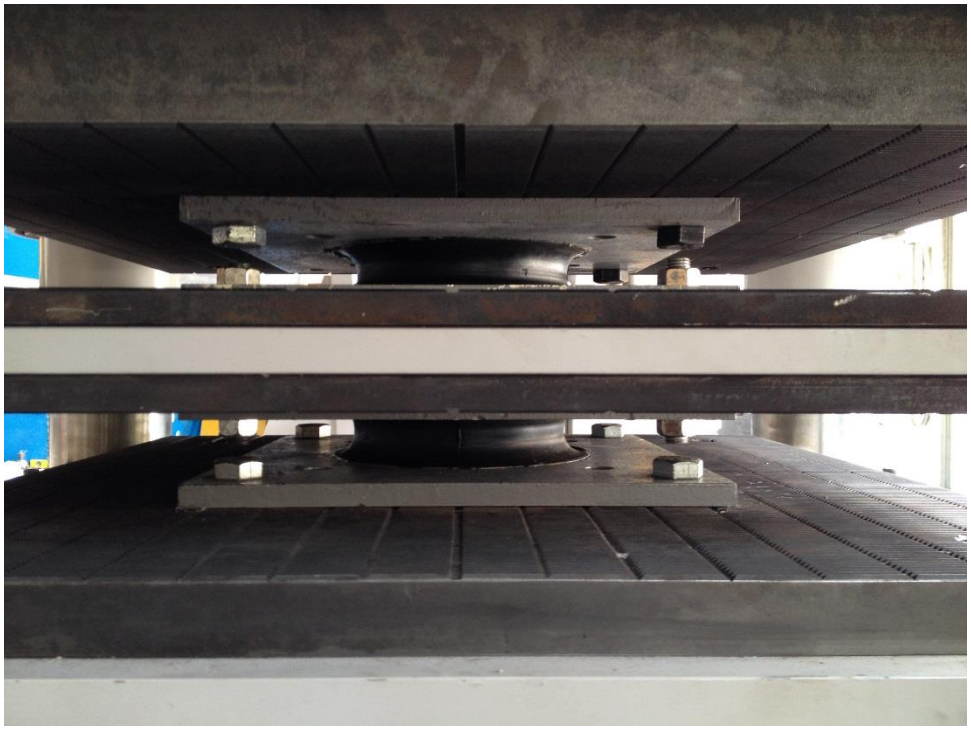

Figure C.3: C-15 bearing in the case of a tension without displacement

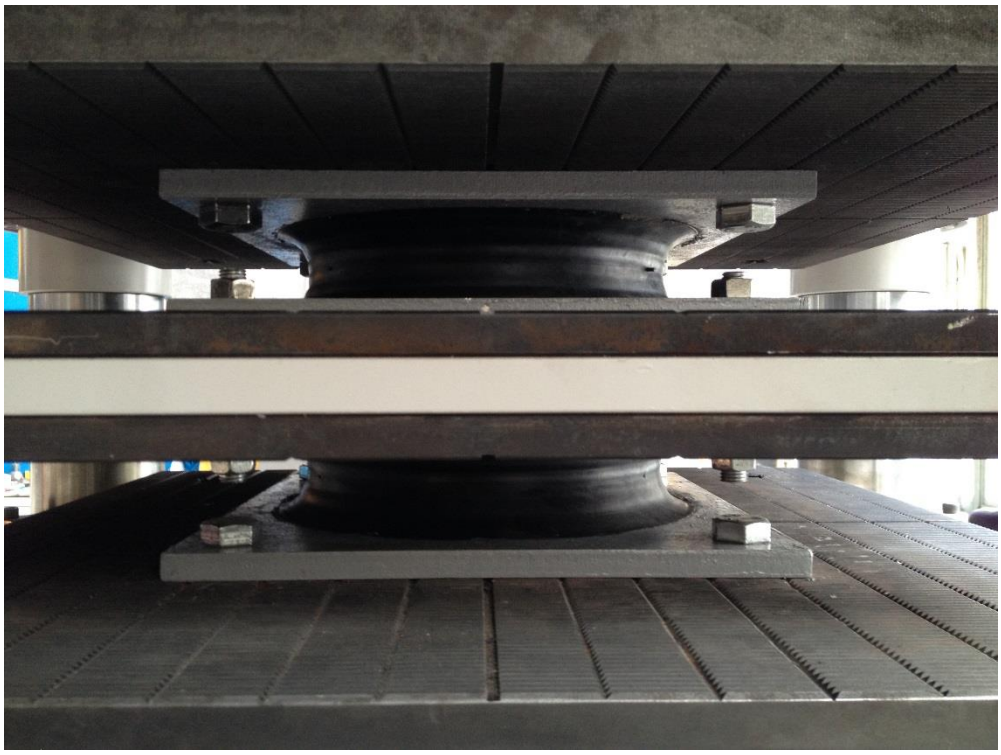

Figure C.4: C-30 bearing in the case of a tension without displacement

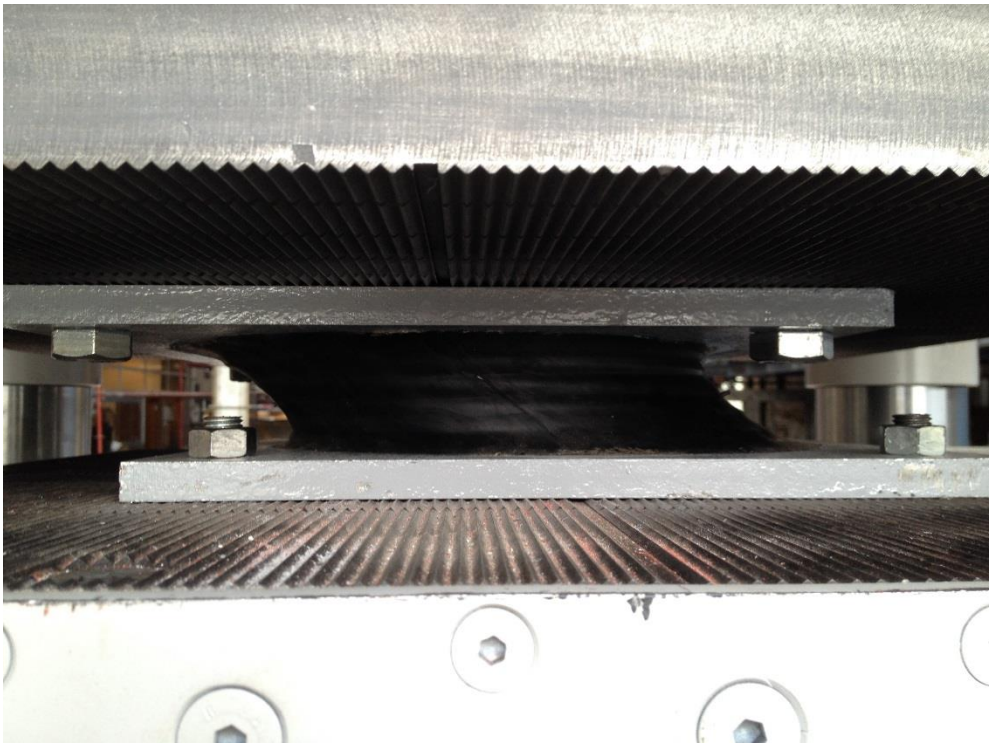

Figure C.5: C-30 bearing in the case of a tension with 100% displacement

Figure C.6: O-15 bearing in the case of pure tension with %0 strain

Figure C.7: O-15 bearing in the case of pure tension with %25 strain

Figure C.8: O-15 bearing in the case of pure tension with %50 strain

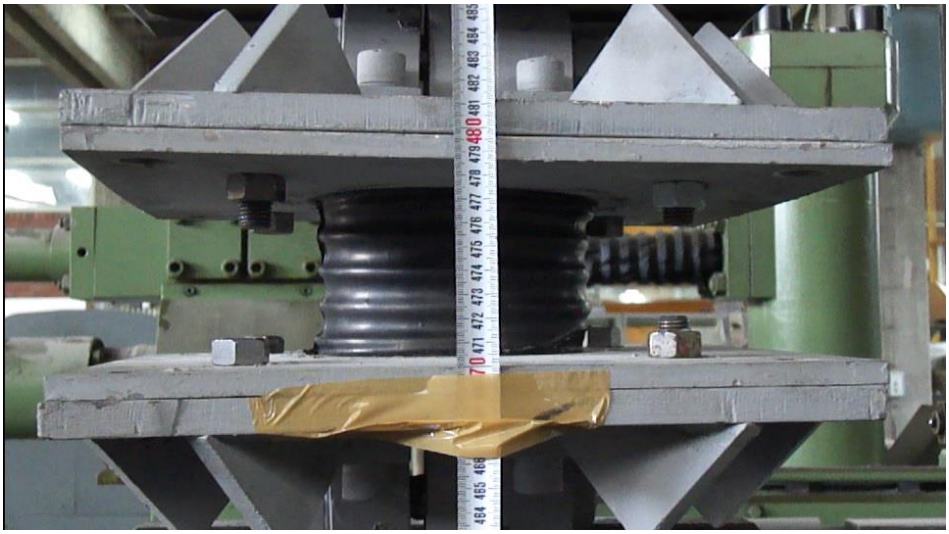

Figure C.9: O-15 bearing in the case of pure tension with %100 strain

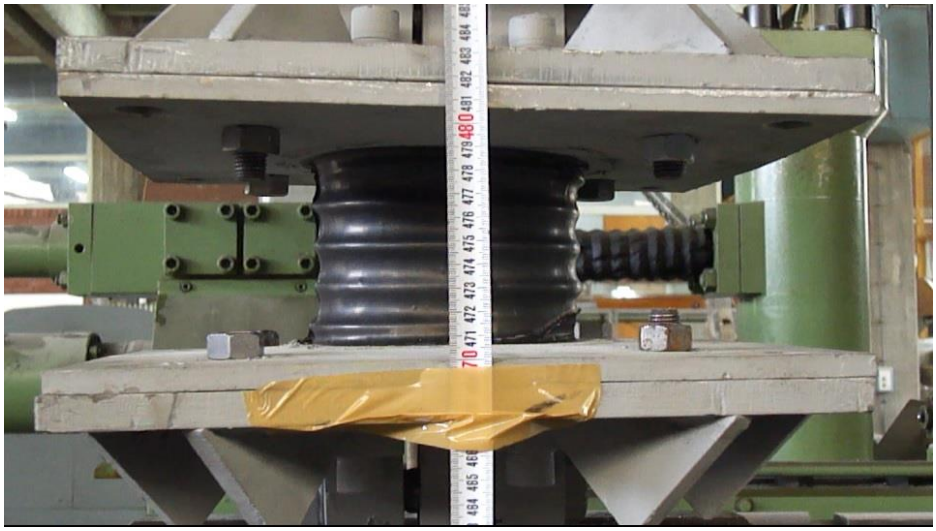

Figure C.10: O-15 bearing in the case of pure tension with %150 strain

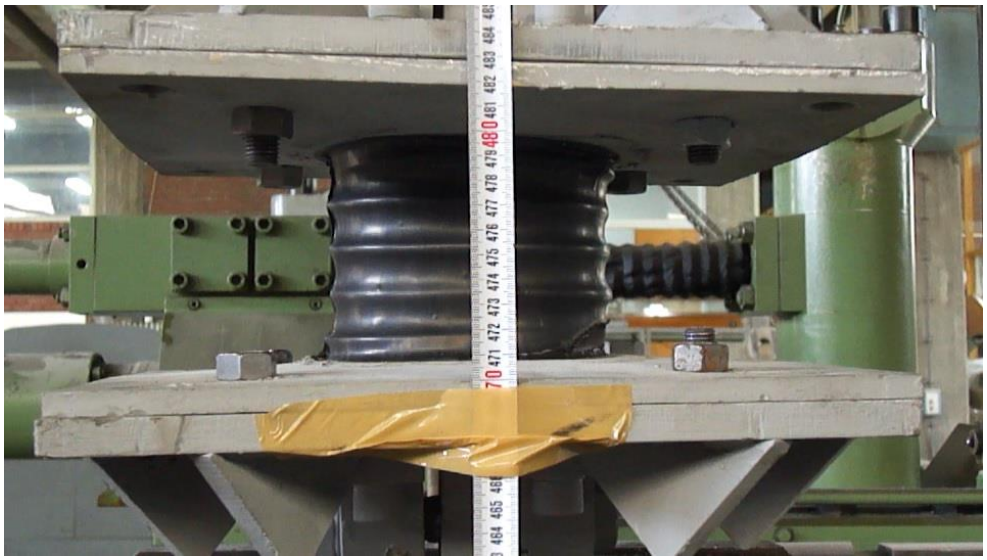

Figure C.11: O-15 bearing in the case of pure tension with %220 strain

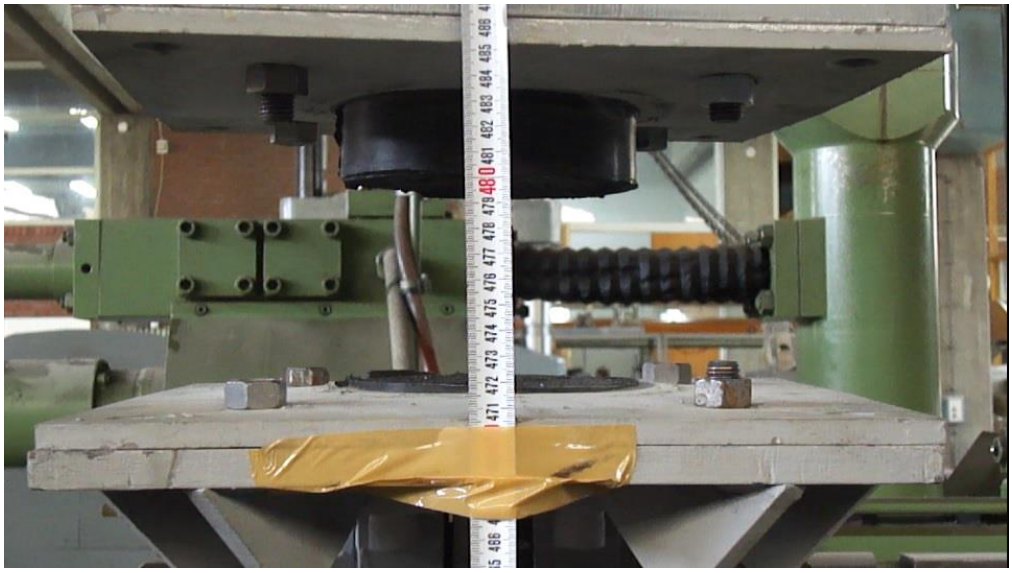

Figure C.12: O-15 bearing in the case of bearing is ruptured

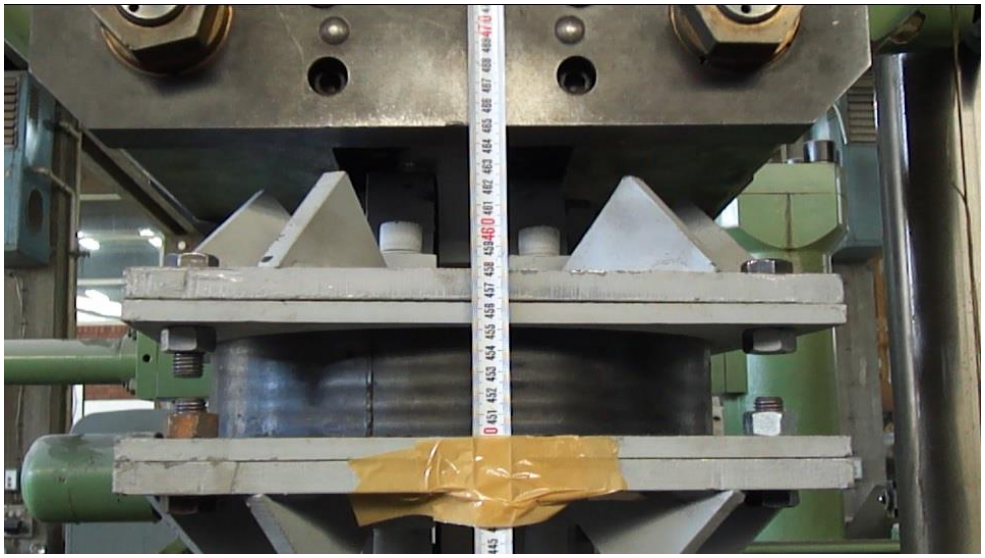

Figure C.13: O-30 bearing in the case of pure tension with %0 strain

Figure C.14: O-30 bearing in the case of pure tension when outer plates are bended

Figure C.15: O-30 bearing in the case of failure

APPENDIX D

ESSENTIAL FEATURES OF BEARINGS

In Appendix D part, tables which are listed specifications of bearings in detail are given. When bearings are designed, AASHTO LRFD (2010, Section 14.7.6) is used.

Table D.1: Physical properties of O-15 bearing

Elastomeric Bearing – O-15			
Input		Output	
Diameter	150 mm	Elastomeric thickness	4 mm
Total height	35 mm	Shape factor	9.375
Number of steel plate	5	Allowable compression load	8.3 tons
Steel plate thickness	3 mm	Allowable tension load	2.1 tons
G	0.4 MPa	Stability	Eligible
Allowable stress	8.62 MPa		Circular

Table D.2: Physical properties of O-30 bearing

Elastomeric Bearings - AASHTO LRFD (2010, Section 14.7.6)			
Input		Output	
Diameter	300 mm	Elastomeric thickness	8 mm
Total height	55 mm	Shape factor	9.375
Number of steel plate	5	Allowable compression load	33.1 tons
Steel plate thickness	3 mm	Allowable tension load	8.5 tons
G	0.4 MPa	Stability	Eligible
Allowable stress	8.62 MPa		Circular